筑　波　大　学

博 士 （医 学） 学 位 論 文

Two histone variants TH2A and TH2B facilitate human iPS cell generation

（２つの異型ヒストン TH2A と TH2B は

ヒト iPS 細胞の作製を促進する）

2015

筑波大学大学院博士課程人間総合科学研究科

HUYNH MY LINH

Acknowledgments

I would like to express my gratitude to my academic supervisor, Professor Shunsuke Ishii, who has given me an exceptional learning oppoturnity. I appreciate his expertise, understanding, patience and guidance.

A very special thanks to Dr. Toshie Shinagawa, without whose instruction, motivation and encouragement I would not have considered a graduate career in stem cell research.

I also would like to acknowledge RIKEN Molecular Genetics Laboratory members for their support throughout my graduate program.

Finally, I would like to thank my family and my partner, whose love and encouragement are always with me.

論　　文　　概　　要 (Thesis Abstract)

○ 論 文 題 目

Two histone variants TH2A and TH2B facilitate human iPS cell generation

（２つの異型ヒストン TH2A と TH2B はヒト iPS 細胞の作製を促進する）

○ 指導教員 (Supervisor)

人間総合科学研究科　生命システム医学専攻　石井俊輔　教授

(Graduate School of Comprehensive Human Sciences, Biomedical Sciences, Shunsuke Ishii)

(所　　属)　　筑波大学大学院人間総合科学研究科 生命システム医学専攻

(Graduate School of Comprehensive Human Sciences in University of Tsukuba, Doctoral Program Biomedical Sciences)

(氏　　名)　　HUYNH MY LINH

ABSTRACT

Purpose

There are two major methods of reprogramming: generation of induced pluripotent stem cells (iPSCs) by overexpressing embryonic-stem-cell-specific transcription factors (OCT4, SOX2, KLF4 and c-MYC) and somatic cell nuclear transfer (SCNT) by oocyte-specific factors. Previously we reported oocyte-enriched histone variants TH2A, TH2B and the histone chaperone nucleoplasmin (NPM2) enhance the reprogramming by OSKM in mice. Mouse histone TH2A and TH2B form unstable nucleosome compared to canonical histones. In this study, I investigated the role of mouse histone TH2A and TH2B in modulating chromatin structure. Moreover I tested the role of human TH2A, TH2B and NPM2 in human induced pluripotent stem cell generation.

Material and methods

TH2A (*HIST1H2AA*, NM_170745.3) and TH2B (*HIST1H2BA*, NM_170610.2) were amplified from genomic DNA by PCR and inserted into pLenti6.3 vector. Expression of TH2A and TH2B were confirmed by western blot. Lentivirus system was used to generate induced pluripotent stem cells. After indicated time, live cell staining was performed with anti-SSEA4 and anti-TRA-1-60 antibodies to count iPSC colonies. In vitro differentiation was performed by transferred iPSCs into non-adherent plate for 3 days prior to spontaneous differentiation in adherent plate. For teratoma formation, single iPSCs were transplanted into dorsal flanks of NOD/ShiJic-scidJcl mice. Teratomas were dissected after six to nine weeks and processed to hematoxylin and eosin staining or immunostaining with antibodies for three germ layers markers. Microarray analysis was performed by Human Gene 1.0 ST Array and processed by R package Oligo.

Results

The nuclei from NIH3T3 cells expressing mouse TH2A, TH2B, and P-Npm exhibited higher DNase I sensitivity than those from cells overexpressing canonical histones. However these histone variants did not affect the total H3K9me3 level. $Th2a^{-/-}Th2b^{-/-}$ spermatids have

defects in the deposition of TNP2 on chromatin. The level of canonical histone H2B is upregulated by a feedback mechanism.

Human TH2A, TH2B and NPM2 enhance the OSKM-induced reprogramming of human dermal fibroblasts and umbilical vein endothelial cells. Pluripotency of iPSCs generated by co-expression OSKM and TH2A, TH2B, NPM2 was shown by *in vitro* and *in vivo* differentiation assays. These iPSCs gave rise to highly differentiated teratomas compared to iPSCs induced by OSKM alone. Genome-wide analysis showed that TH2A, TH2B and NPM2 regulated genes which are involved in naïve stem cell stage. Thus, TH2A, TH2B and NPM2 enhance reprogramming of human somatic cells and improve the quality of human iPSCs

Discussion

Open chromatin is a hallmark of ESCs and iPSCs, in which the overall genome is hyperactive and the levels of heterochromatin are reduced compared with differentiated cells. The open chromatin state in ESCs is maintained by multiple chromatin remodeling factors, including Chd1 and the TIP60-p400 complex. Reduction of the Chd1 level in ESCs increased the amount of heterochromatin, whereas expression of TH2A/TH2B did not affect the level of H3K9me3, a typical marker of heterochromatin. These results suggest that TH2A/TH2B contribute to the reprogramming of somatic cells by inducing transcriptionally active open chromatin, whereas Chd1 contributes to the maintenance of an established open chromatin state in ESCs by suppressing heterochromatin formation.

During the transition stage histone-to-protamine of spermiogenesis, multiple mechanisms may act in combination to destabilize the nucleosome and replace the histones. Hyperacetylation of canonical histones during spermatogenesis, especially H4, and multiple histone variants are thought to weaken DNA–histone octamers and nucleosome–nucleosome interactions. Nucleosomes containing hyperacetylated histones are thought to be more prone to displacement by protamines. These previous reports are consistent with the observations

that mouse TH2A/TH2B, which induce an open chromatin structure, are required for the replacement of histones by TNPs.

The effect of BAN is depend on the cell type of origin. BAN can enhance the number of TRA-1-60 and SSEA-4 positive colony number in HUVECs about 8 fold and 3.5 fold respectively. On the other hand, the degree of enhancement for adult dermal fibroblast is approximately 2.5 fold. During the reprogramming process, chromatin is reorganized and open chromatin structure is formed. HUVECs may efficiently form open chromatin than adult fibroblasts. BAN-regulated genes are overlapped with transcript signature of naïve human ESCs. Open chromatin structure induced by BAN may facilitate the naïve state of human ESCs or iPSCs. Indeed Ware et al. (2014) reported human ES cell lines in the later primed state can be toggled in reverse to naïve by exposure to histone deacetylase inhibitors prior to naïve culture. Naïve state cells are showed to have a high cellular potency due to the genome wide low methylation levels, and low expression of lineage specific genes, however mechanisms underlie the naïve state is still unclear and how BAN involve in this naïve state is an interesting topic for further research

Conclusion

In summary, TH2A and TH2B induce an open chromatin structure. The addition of TH2A, TH2B and P-NPM2 in the reprogramming cocktail may be a useful tool for generating clinical grade human iPSCs effectively.

Table of contents

List of tables and figures

Figure No. Figure Title Page No.

CHAPTER 1. INTRODUCTION

1.1 Overview of cellular potency

The development starts from zygote, which has the highest cellular potency. Zygotes and early embryonic blastomeres up to four-cell embryonic stages are totipotent (Tarkowski et al., 1959) (Figure 1.1). These totipotent cells can differentiate into any cell types including embryonic and extraembryonic cell types. At the 16-cell stage, mouse embryonic blastomere separates into two lineages: the trophoblast lineage, which will develop to a part of placenta; and the inner cell mass (ICM) which gives rise to the epiblast and the hypoblast. The epiblast lineage cells will develop into the embryo, which consists of all the somatic cells and germline cells.

Mouse embryonic stem cells (ESCs) (Evans and Kaufman, 1981; Martin, 1981) can be derived from expanding the ICM *in vitro*. These ESCs are pluripotent, they can form full embryo when aggregate with early blastomeres.

After implantation into uterine wall, the late blastocyst converts into a cup-shaped structure known as egg cylinder (Kaufman, 1992). This egg cylinder is subjected to a systematic topological changes guided by growth factors from yolk sac and trophoblast cells (Beddington and Robertson, 1999). Transplantations of egg cylinders experiments indicate that they still can change fates (Gardner and Beddington, 1988). However, postimplantation epiblast stem cells can not contribute to embryo in chimera assay (Rossant, 2008). Therefore epiblast stem cells (EpiSCs) derived from post implantation blastocyst are primed pluripotent stem cells, which are primed to differentiate into specific cell types (Nichols et al., 2009).

Human embryonic stem cells have been derived from human blastocysts (Thomson et al., 1998). However these human ESCs are significantly different from mouse ESCs in term

of morphology, differentiation capacity, transcriptional profiles and culture requirements. Human ESCs cannot contribute to embryo in chimera assays. The highest pluripotency test for human ESCs is based on teratoma formation, when they are injected into nude mice. Thus human ESCs are thought to be the analogous to mouse EpiSCs (Brons et al., 2007, Rossant, 2008 and Tesar et al., 2007).

Recent studies show that human ESCs can be converted into a naïve state, which is more similar to mouse ESCs, however still somewhat contradictory and controversial (Chan et al., 2013; Gafni et al., 2013; Takashima et al., 2014; Theunissen et al., 2014; Ware et al., 2014). By using different modified culture medium or genetic modification by overexpressing key naïve transcription factors, the naïve hESCs transcriptional network is resetted to a more similar degree with their counterpart in early blastocysts stages. They also can contribute to chimera assay, exhibit low DNA methylation, and better differentiation capacity compared to primed ESCs.

1.2 Reprogramming in early embryo

Oocyte and sperm are one of the most highly specialized cells in the body. Upon fertilization, these gametes must undergo a drastic reconfiguration to form the zygote, which possesses the highest pluripotency. This remodeling involves both paternal and maternal genomes. In mammal, the oocyte is ovulated at the second meiotic metaphase and completes the meiosis when fertilization occurs, which results in the formation of a maternal pronucleus and a second polar body. On the other hand, the sperm genome is tightly packaged with nucleoprotamine, upon fertilization, the sperm nuclear envelope is broken down, protamines are exchanged with histones, then chromatin is decondensated and pronuclear is formed (Dean et al., 2003).

1.3 Induced pluripotent stem cells

In 2006, Takahashi and Yamanaka successfully convert mouse somatic fibroblasts into induced pluripotent stem cells (iPSCs) by overexpressing four transcription factors: Oct4, Sox2, Klf4, and c-Myc (Takahashi, 2006). These iPSCs can contribute to both somatic and germline in chimeric mice (Okita et al., 2007 and Wernig et al., 2007), which are the hallmark of ESCs. These factors trigger stochastic events which lead to the reactivation of endogenous pluripotent genes such as Oct4, Nanog, Sox2, from which an auto-regulatory network is established and support the pluripotent state independent of transgenes.

Since the discovery of iPSCs, different strategies are used to induce reprogramming, however only a small fraction of donor cells can be successfully induced to iPSCs. Thus the reprogramming efficiency seems to be very low. There are several key events which are thought to link to reprogramming efficiency such as cell division rate and chromatin structure.

Inhibition of p53/p21 pathway or overexpression of Lin28 enhance iPSCs generation proportionally to the increase in cell division rate (Kawamura et al., 2009; Lapasset et al., 2011). These observations suggest that accelerated cell division may increase the number of donor cells, of which each daughter cell has an independent chance to become iPSC, or DNA replication is necessary for epigenetic alteration, such as histone and DNA modifications.

Another barrier of reprogramming is chromatin structure (Gaspar-Maia et al., 2011). The term chromatin was proposed by Walther Flemming in 1882 which means stainable material. In 1928, Emil Heitz defined heterochromatin and euchromatin based on differential compaction in interphase nuclei. Heterochromatin is more densely stained, compacted, in contrast to euchromatin, which are sparsely stained. Compared to somatic cells, ESCs have a loosen chromatin structure, euchromatin is more abundant compared to heterochromatin than in differentiated cells. In reprogramming assay, the addition of agents which boost chromatin

decondensation such as DNMT (DNA methylatransferase) inhibitor 5 aza-cytidine, HDAC (Histone deacetylase) inhibitor valproic acid leads to increased reprogramming efficiency (Mikkelsen et al., 2008; Huangfu et al., 2008). Overexpression of chromatin remodeling complexs such as BAF family components BRG1 and BAF155 (Singhal et al., 2010) also promote the reprogramming process. These evidences suggest that re-opening chromatin during reprogramming is a key event and promote the opportunity for activating the transcriptional network of pluripotency.

Even though overexpression of four transcription factors OSKM are able to convert somatic cells into iPSCs, the overall efficiency is still very slow, which cause a difficulty in understanding the molecular mechanism. It has been shown that reprogramming by OSKM is a step-by-step process, which involves an early stochastic phase and a deterministic phase. At the early stochastic phase, somatic cells have variable latencies, then partially reprogrammed cells will go through a hierarchal process to reach pluripotency.

Since the discovery of OSKM, many groups have tried to substitute these four transcription factors by other factors. Among them, c-Myc is the first factor which is dispensable and can be replaced by n-Myc, I-Myc or maternal transcription factor Glis-1 (Wernig et al., 2008; Nakagawa et al., 2008, Maekawa et al., 2011). Nuclear receptor Nr5a2 and Nr5a1 can replace Oct4 when combined with KSM (Heng et al., 2010). Sox7 and Sox17 can replaced Sox2 by modified a mutation in the High-Mobility-Group (HMG) DNA-binding domain which in turn promotes the binding of Oct4 to canonical Oct-Sox site (Jauch et al., 2011; Aksoy et al., 2013). Esrrb (Estrogen-related receptor beta) is highly expressed in ES cells, can substitute Klf4 (Feng et al., 2009).

Many chemical approaches also show that small molecule compounds can promote reprogramming and replace some or all four factors OSKM. Trichostatin A (TSA), valporic acid (VPA), butyrate, and suberoylanilide hydroxamic acid (SAHA) are histone deacetylases

inhibitors, which can facilitate the reprogramming process and replace c-Myc (Huangfu et al., 2008; Mali et al., 2010; Esteban et al., 2010; Blaschke et al., 2013; Stadtfeld et al., 2012). Oct4 can be substituted by Forskolin, which is a cAMP agonist. The combination of CHIR99021 (a GSK-3 beta inhibitor), 616452 (TGF-beta RI kinase inhibitor II), Forskolin and DZNep (S-adenosylhomocysteine hydrolase inhibitor) is able to reprogram mouse somatic cells into iPSCs (Hou et al., 2013). Although this cocktail is able to produce iPSCs in mice, it fails to induce human cells into iPSCs. These studies indicate that the small compound molecules can induce a global open chromatin structure, which assist the reprogramming role of OSKM.

After OSKM are overexpressed, they bind to the genome at many nonfunctional sites, due to the high level of overexpressed proteins (Soufi et al., 2012). These nonfunctional sites are different from the core OSK targets *in vivo*, however OSKM also bind near genes which facilitate the "on-target" and prevent the "off-target" of the reprogramming process. These observations suggest that OSKM not only open up the road to pluripotency but also to other cell fates such as cardiogenesis and neurogenesis or apoptosis. This unrestrained binding mode of OSKM initially lead to a stochastic phase prior to transitioning to a more deterministic phase.

At first, OSK bind to distal elements of repressed genes due to the inaccessibility to promoter regions of these genes. Among four factors OSKM, c-Myc is not a pioneer factor. c-Myc binds to OSK and enhance the accessibility of OSK to their targets, which in turn amplify the gene expression. Chromatin remodeling complex BAF has been reported to enhance the accessibility of Oct4 to promoters and increase the reprogramming efficiency without c-Myc (Singhal et al., 2010). In line with the positive effect of chromatin modifier BAF, KDM2A and KDM2B are H3K36me2 demethylases; UTX, an H3K27 demethylase; WDR5, an "effector" of H3K4 methylation are able to induce open chromatin and increase

reprogramming efficiency (Ang et al., 2011; Mansour et al., 2012; Pijnappel et al., 2013). In brief, the stochastic events driven by OSKM can be enhanced by inducing global open chromatin structure to facilitate the accessibility of OSKM to target genes.

Follow the initial stochastic phase, a small number of successfully converted cells enter a deterministic step. Using the single cell expression profile approach, reactivation of endogenous Nanog and Sox2 are predictive of a deterministic pluripotent fate (Buganim et al., 2012). Moreover, the reactivation of endogenous Gdf3, Dppa2, Dppa3 (Stella) are markers for stablization of pluripotency (Golipour et al., 2012). Interestingly, these stabilization marker genes are located in a megabase-scale chromatin domains spanned by H3K9me3, which is not accessible in fibroblasts. In conclusion, OSK binding sites are rearranged to resemble the *in vivo* "on-target" sites.

The chromatin structure of somatic cell is a major target for facilitating reprogramming. Knocking down SUV39H1/H2, H3K9 methyltransferases, significantly increase the reprogramming efficiency by removing heterochromatin domain which blocks OSKM binding to pluripotent genes (Onder et al., 2012; Sridharan et al., 2013). At the final phase of reprogramming, BMP signaling arrests the reprogramming cells in pre-iPSCs by inducing high level of H3K9me3. The same study also shows that Vitamin C can reduce H3K9me3 level and facilitate the conversion of pre-iPSCs into iPSCs (Chen et al., 2012). Depletion of MBD3, a component of NuRD repressor complex, results in a deterministically reprogramming process, in which 95% cells are converted to iPSCs (Rais et al., 2013). At the same time, other groups showed that depletion of MBD3 only enhance reprogramming moderately (0.15% to 1.5%) (Lou et al., 2013). The high efficiency reported can be due to the effect of secondary system reprogramming and medium which contains inhibitors of GSK3-beta and MEK kinases. At the initial stage, MBD3 seems to be recruited by OSKM at the "off-target" sites to form heterochromatin, which blocks the reprogramming process.

Therefore, knocking down of MBD3 may synchronize cells at early stochastic phase (Soufi et al., 2014).

1.4 Reprogramming by nuclear transfer

Reprogramming of somatic cells by nuclear transfer (SCNT) was originally demonstrated by injection nuclei of somatic cells into enucleated Xenopus oocytes (Gurdon et al., 1958). Since then, reprogramming of mammalian cells by nuclear transfer has been successfully done in sheep (Wilmut et al., 1997), mouse (Wakayama et al. 1998) and human (Noggleet al., 2011).

These studies indicate the presence of reprogramming factors in oocyte, which influence the epigenome of somatic cell nuclei and reprogram it toward the totipotent state. However the molecular events and factors that occur during SCNT are unclear. Recently Jullien et al. (2014) shows that mouse somatic nuclei is reprogrammed into an oocyte gene expression pattern, rather than that of ESCs or ICM. Moreover reprogramming is independent of DNA synthesis and cell cycle replication as previously known.

In contrast to current protocols for direct reprogramming by Yamanaka four factors, reprogramming by SCNT appears to happen in a single event. Moreover, SCNT give rise to fully reprogrammed pluripotent cells with no trace of partially reprogrammed cells found in iPSC approach (Hasegawa et al., 2010). ESCs derived from SCNT embryo have less epigenetic abnormalities compared to iPSCs (Ma et al.,2014).These observation suggests that reprogramming by SCNT is a synchronized process in contrast to stochastic processes induced by Yamanaka four factors.

1.5 Current advances of human iPSCs and implications

After Yamanaka's discovery of iPSC generation by overexpressing four transcription factors, numerous studies have been done to overcome the limits of low efficiency, safety and quality of iPSCs. Firstly, some technical developments have been developed following the original viral delivery, which focus on eliminating transgene integration and simplifying the methods to achieve high expression of transcription factors. For example: episomal vectors, piggyBac transposon, recombinant proteins, minicircle vectors, synthetic mRNA, and so on. Depending on the application purpose, the most safety approaches for generating clinical grade human iPSCs is recombinant protein. On the other hand, for studying the process and mechanism of reprogramming, dox-inducible Piggybac transposon or lentiviral constructs are the most robust systems. Second concern about generating human iPSCs is the low efficiency of the process. For this area, researches are focused to dissecting the mechanism of reprogramming or identify new factors which can augment the process. Recently findings indicate that some transcriptions factors, such as Glis-1, L-Myc, and Nr5a2, cell cycle regulators, such as p53 and Ink4a locus, and chromatin modifiers, such as VPA and vitamin C, or noncoding RNA, such as lincRNA-ROR and mir-302, can enhance the reprogramming efficiency in human cells. The third and most important aspect is the quality of iPSCs. In testing drugs or regenerative medicine, iPSCs will be induced to differentiate into desired cell types before application. Therefore the most important characteristic of iPSCs is the capacity to differentiate into any cell types. Some reports have shown that iPSCs have memories and easy to be converted into original cell types (Lister et al., 2011; Ohi et al., 2011; Bar-nur et al., 2011). Bar-nur et al. (2011) evaluated the level of histone H3 acetylation in iPSCs derived from beta cells and non-beta cells. They found acetylated H3 at Insulin and Pdx1 genes in beta cell-derived iPSCs, even though both genes are not expressed, but not in non-beta cell

derived iPSCs or ESCs. The retained memories may cause low differentiation efficiency and aberrant phenotypes in differentiated cells derived from iPSCs.

1.6. Spermatogenesis

The seminiferous tubules contain germ cells and somatic Sertoli cells (Hess et al., 2008). The Sertoli cells create a microenvironment, which are necessary for maintaining the production of spermatozoa. Blood and lymphatic vessels and Leydig cells locate in between the seminiferous tubules. These support cells produce growth factors, which are important for the development of germ cells. On the other hand, the myoid cells are structural support, which have a role in fluid and sperm movement through the lumen of seminiferous tubules. The spermatogenesis process can be divided into three phase: mitotic phase, meiotic phase and spermiogenesis.

The spermatogonial stem cells located at the basement of the seminiferous tubules. These single spermatogonial cells are called (A_s) (A single) spermatogonia. A_s spermatogonia have the ability to self-renewal, which can generate spermatogonial stem cells in order to preserve the stem cell resource. At the same time, A_s spermatogonia can divide into differentiating spermatogonia, which will go through differentiation process and finally fully differentiated germ cells so called sperms.

One A_s spermatogonium divides into two differentiating spermatogonia which are interconnected via an intercellular bridge. These A_{pr} (A paired) spermatogonia can undergo mitotic divisions, which result in a 4, 8, 16, or 32 A_{al} (A aligned) spermatogonia. A_{al} spermatogonia differentiate without mitotic division into A_1 spermatogonia. A_1 spermatogonia undergo mitotic divisions to form series of A_2, A_3, A_4, Intermediate and B spermatogonia. B spermatogonia divide mitotically to form primary spermatocytes.

Primary spermatocytes start the first meiotic division (M-I), which give rise to secondary spermatocytes. Subsequently, the second meiotic division (M-II) occurs and four haploid round spermatids are produced from one primary spermatocyte. The spermiogenesis can be subdivided into 16 steps based on the morphology. Steps 1-8 contain round spermatids, steps 9-16 contain elongating spermatids. Because the spermatogenesis is well-controlled in a time regulated manner, the stages of seminiferous tubules can be classified into twelve (I-XII) stages based on the developing germ cell types exist.

Transition protein TNP1 and TNP2 have vital role in nuclear condensation during spermiogenesis. They constitute 90% of the chromatin proteins during the histones to protamines transition stages. Knock-out of either TNP1 or TNP2 result in a moderate defect in spermatogenesis, while double knock-out mice are sterile (Yu et al., 2000; Shirley et al., 2004).

1.7 Histone replacement during spermiogenesis

During the elongation phase of spermatogenesis, nuclear chromatin is condensated and transcription is suspended. The most important event during this phase is the replacement of core histones by transition proteins (TNPs) and finally protamines (PRMs). Recent studies indicate that histone modifications such as phosphorylation, ubiquitination or hyperacetylation are involved. Monoacetylated and low levels of diacetylated histone H4 are enriched in stages which associated with histone deposition or transcriptional active stages. Meanwhile, the highly acetylated histones H4 are enriched at the replacement stage (Meistrich et al., 1992). Histone ubiquitination has been linked to nucleosome removal during the post meiotic phase. Recent work showed that histone ubiquitine by ubiquitin ligase RNF8 may induce H4K16 acetylation, which facilitate the removal of histone during transition

stages (Lu et al., 2010). SSTK is a small serine/threonine kinase, which phosphorylate histones H1, H2A, H2AX, and H3. SSTK null mice have defect in elongating spermatids, at the stage of histones to transition proteins replacement (Spiridonov et al., 2005). These observations suggest that TNP1 and TNP2 share overlapping functions. Tnp-null mice also show abnormal protamine 2 processing, which result in the abnormal ratio of protamine 1 and protamine 2 (Meistrich et al., 2003). Protamines are arginine-rich, DNA-binding proteins in the nucleus of vertebrate sperms. These small proteins pack the sperm DNA in a volume less than 5% of ordinary somatic cell nucleus. A reduction in the amount of either protamine 1 or protamine 2 disrupts the nuclear condensation process (Cho et al., 2001; Jan et al., 2012).

1.8 Histone variants and cellular plasticity

In eukaryote, DNA is wrapped around core histones to form chromatin, which then folded and packed into chromosome. There are 4 core histone proteins: histone H3, histone H4, histone H2A and histone H2B, together they form an octamer. Canonical histones are synthesized in coordination with DNA replication, while histone variants are non-allelic isoforms of canonical histones. Many evidences showed that histone variants are produced in order to replace canonical histones during cellular transition. Histone variants H2A.Z, and H3.3 facilitate cellular plasticity in early development. Histone variants H2A.X, H3.3, and macroH2A inhibit developmental plasticity following cellular differentiation. Variants H3.3, H2A.Z, and H2B.E regulate cellular plasticity in the adult nervous system (Santoro et al., 2015).

Prior to the deposition of histones into chromatin, and after removal from chromatin, these histones are soluble. Histones are basic proteins, which easily interact with other acidic partners, and these interactions may form non-desired aggregations. In order to protect cells

from such defects, histones are usually associated with factors known as histone chaperones, which can buffer the positive charge. Nucleoplasmin is the first identified histone chaperone which involved in the prevention of histone-nucleic acid aggregation.

Nucleoplasmin was purified from *Xenopus lavevis* oocytes in 1978. Nucleoplasmin functions as a storage pool for histone H2A and H2B dimers. On the other hand, N1 and N2 proteins are storage pool for histone H3 and H4 dimers. In vertebrates, there are three members of nucleoplasmin (NPM1, NPM2, and NPM3). Npm2 forms a homopentamer structure which contains five individual 22kDa subunits. Amino acids 16 to 120 form core domain for pentamerization and heat stability. NPM2 is phosphorylated in oocyte and heavily phosphorylated at meiosis II. This hyperphosphorylation modification is essential for DNA decondensation and exchange of protamine of paternal DNA at zygote stage. The phosphomimic form of NPM2, in which serine is converted to aspartate showed an enhance affinity for histone H2A-H2B dimers (Gurard-Levin et al.).

Recently we found that mouse TH2A and TH2B (*Hist1h2aa* and *Hist1h2ba*) help to establish developmental plasticity in the early embryo (Shinagawa et al., 2014). Histone variants TH2A and TH2B, which differ from canonical H2A and H2B by 15 and 16 amino acids, respectively, were first identified in mammal testis (Trostle-Weige et al., 1982; Shires et al., 1976). TH2A and TH2B are highly expressed in oocyte and zygote and gradually decreased as differentiation proceeds to blastocyst stage (Figure 1.2)

Interestingly, TH2A/TH2B double mutant oocytes showed significantly reduced ability to develop to blastocyst stage following fertilization compared to wild-type oocytes. Moreover the paternal genome activation was shown to be defected in zygotes derived from double mutant oocytes. Therefore TH2A and TH2B are maternal effect factors.

Indeed overexpressing of TH2A and TH2B with OSKM in mouse embryonic fibroblasts carrying Nanog-GFP enhance the generation of GFP positive iPSCs (Figure 1.3).

Nucleoplasmin (Npm) is a histone chaperone, which is highly expressed in oocytes (Laskey et al., 1978; Mills et al., 1980). Npm decamer binds to histone octamer, and functions in both storage and deposition of histone octamers onto DNA. After fertilization, Npm contributes to the decondensation of sperm chromatin (Philpott et al., 1991). It was reported that Npm is heavily phosphorylated during fertilization (Bañuelos et al., 2007). As expected, coexpression of phosphorylated form of Npm (P-Npm), TH2A, TH2B and OSKM significantly enhanced the OKSM-induced iPSC generation by approximately 18-fold (Figure 1.3).

We also found that TH2A, TH2B induce an open chromatin by comparing the structural features of nucleosomes containing canonical histones or TH2A/TH2B. The number of strong hydrogen bonds in the nucleosomes containing TH2A/TH2B are decreased compared with nucleosomes containing canonical histones, which suggests a more open chromatin structure exists TH2A/TH2B containing nucleosomes.

Interestingly, TH2A/TH2B enhance the iPSC generation from *Xist* mutant MEFs compared to wild-type MEFs. A previous study showed that cloning efficiency of *Xist* mutant nuclei by SCNT was much higher than that of wild-type nuclei (Inoue et al., 2010). Thus, the addition of TH2A/TH2B to the somatic cell reprogramming process leads to greater similarity to oocyte-based reprogramming and SCNT (Figure 1.4).

CHAPTER 2. THE ROLE OF MOUSE HISTONE VARIANTS TH2A AND TH2B IN CHROMATIN CONFIGURATION

2. 1 RESEARCH PURPOSE

Mouse histone variants TH2A, TH2B and P-Npm2 enhance the reprogramming process induced by OSKM (Shinagawa et al., 2014). TH2A and TH2B are highly express in oocyte and testis, which indicate they may function in oogenesis and spermatogenesis. Th2a/Th2b double mutant male mice are sterile (Shinagawa et al., 2015). In this study, the role of two histone variants TH2A, TH2B in chromatin configuration is investigated in two contexts:

1. The role of TH2A and TH2B in reprogramming process through characterization of the chromatin features of NIH3T3 cell line overexpressing mouse TH2A, TH2B and P-NPM2.

2. The role of TH2A and TH2B in chromatin configuration of spermatids using mutant mice lacking both TH2A, TH2B.

2.2 MATERIALS AND METHODS

Animal

Th2a/Th2b-deficient mice were generated as described (Shinagawa et al.,. 2014). Mutant mice were backcrossed with BALB/c mice five times or more before use in the experiments.

Immunohistochemical examination of testes

Testes and caput epididymis were fixed in Bouin's solution overnight, embedded in paraffin, and sectioned. Sections were used for hematoxylin and eosin staining, periodic acid Schiff (PAS) staining, and immunofluorescence. For immunostaining, sections were subjected to antigen retrieval and stained with an anti-TNP2 antibody (Santa Cruz Biotechnology) or an anti-γH2AX antibody (Millipore). The secondary antibodies were Alexa Fluor 488- or Alexa Fluor 568-conjugated anti-goat or anti-mouse IgGs (Invitrogen).

Preparation of testicular cells

The testes of two adult mice (8–12 weeks old) were dissected, and the seminiferous tubules were released during a 15 min incubation at 37°C in 1 ml of RPMI medium containing 1 mg/ml of collagenase (Sigma). The tubules were then allowed to sediment, the medium replaced by 1 ml of the RPMI without collagenase, and then washed three times with 1 ml of RPMI. To make a tubular segment, the resulting sediment was incubated for 15 min at 37°C in 1 ml of trypsin solution (50 µl/ml in RPMI; Invitrogen). After adding fetal bovine

serum (FBS) to a final concentration of 10%, the germinal and Sertoli cells were released by pipetting and filtered through 70 µm pore filters (Becton Dickinson).

Isolation of round and elongated spermatids

Velocity sedimentation at unit gravity (STA-PUT gradient) was used to isolate spermatocytes, round and elongated spermatids as described (Bryant *et al.* 2013; Romrell *et al.* 1976)**.** Apparatus was assembled according to the protocol. A linear gradient was generated from 275 ml of RPMI medium added with 2% and 4% BSA. Thirty m*illiliters* of RPMI medium containing 0.5% BSA were loaded into the loading chamber, followed by ten m*illiliters* of testicular cells. After 3 hours of sedimentation, cells were collected in each fraction of 14-ml, and numbered as Fraction #1 from the beginning. Fractions were examined under microscope. Three first fractions were omitted because of containing heterozygous cell population or big cell clumps. Spermatocytes were usually enriched from Fraction # 4-9, round spermatids were from 13-18, and elongated spermatids were from 22-27. Fractions containing cell of interest were pooled and collected by centrifugation at 500 x g for 10 min.

Separation of chromatin and non-chromatin fraction

Whole cell extracts, chromatin fraction or non-chromatin fraction from testicular cells were used for Western blotting. To separate chromatin and non-chromatin fraction, cells were suspended in 5 volume of NETN buffer (50 mM Tris-HCl, pH 8, 100 mM NaCl, 2 mM EDTA, 0.5% NP40) for 15 minutes. The pellet and supernatant were separated by centrifugation and adjusted to the same volume with sample buffer. After electrophoresis and transfer of the proteins to membranes, the membranes were incubated with the indicated antibodies and washed in PBS or 0.5% Triton X-100 containing PBS (only for experiments using anti-TH2B). The signals were detected using ECL Western Blotting Detection

Reagents (GE Healthcare). The following primary antibodies were used: anti-H2A (1:1,500; Abcam), anti-H2B (1:2,000, Millipore) anti-TH2A (1:9,000), anti-TH2B (1:5,000), and anti-H3 (1:10,000; Abcam), anti-H4 (1:1,250; Millipore), anti-protamine 2 (1:300, Santa cruz), anti-H3K14ac (1:3,000, Epigentek), anti-actin (1:3,000, Santa cruz).

qRT - PCR

Total RNA was isolated using Isogen (Nippon Gene). qRT- PCR was performed using SuperScript III Platinum SYBR Green One-Step qRT-PCR kit (Invitrogen). Primer sequences are shown in Table 2.1

Table 2.1

qRT-PCR		
Gene	Forward	Reverse
TNP2	CCGTGCACTCTCGACACTCA	CCTTCAAAGGTCTTCCTGTTCTTG
Ube2a	ATCCTAACGTCTATGCAGATGGT	CGCTTTTCATATTCCCGCTTGTT
Rnf12	CAGCTCAGCGCAGAAGTCAA	TGTGGTGGTGGACCCTCTTT
Prm1	GGCCAGATACCGATGCTGCCG	ATCGCCTCCTCCGTCTGCGA
FoxJ1	CTTCCGCCATGCAGACCCCA	AGCAGGCGCTCTGCGTACTG
TPAP	CCCCTCGCGCCTTCGGATCA	GCCAGGCTGATGGGGGACGA
Gapdh	ACTGGCATGGCCTTCCG	CAGGCGGCACGTCAGATC

DNase I Sensitivity

NIH3T3 cells stably expressing H2A, H2B, and P-Npm, or TH2A, TH2B, and P-Npm, were established by retroviral infection. After infection, the cells were selected and maintained in medium supplemented with 400 μg/ml G418 (Calbiochem). Nuclei were isolated from NIH3T3 cells essentially as described by Rao et al. (1983). Briefly, cells were harvested and homogenized in buffer A (10 mM Tris-HCl, pH 7.5, 5 mM $MgCl_2$, 1 mM $CaCl_2$, and 40 mM NaHSO3) containing 0.34 M sucrose. After centrifugation, the nuclear pellet was obtained, washed in buffer A containing 0.34 M sucrose, and suspended in 3 ml of the same buffer. The sample was overlaid on 2 ml of buffer A containing 1.8 M sucrose and

centrifuged at 13,500 rpm for 19 min at 4 °C in a Beckman SW55Ti rotor. The nuclear pellet was washed sequentially once each with 1 M and 0.34 M sucrose in buffer A. The washed nuclear pellet was suspended in suspension buffer (50 mM Tris-HCI, pH 7.4, 25 mM KCl, 5 mM $MgCl_2$, 0.1 mM PMSF, and 0.1% Triton X-100) and centrifuged. The resulting pellet was washed once with digestion buffer (10 mM Tris-HCI, pH 7.4, 10 mM NaCl, 5 mM $MgCl_2$, 0.1 mM PMSF, and protease inhibitor cocktail) and stored at 4°C until use. Digestion was carried out in the same buffer at a nuclear concentration of 1.6 A260 units/ml (measured in 2 M NaCl and 5 M urea) with 0.0563 U/µl of DNase I (Promega) at 37 °C, as described by Miesky (1971). Digestion kinetics were followed by measuring at 260 nm the amount of DNA that was soluble in 0.166 M perchloric acid and 0.166 M NaCl. The experiment was repeated three times using three independent samples. The data were analyzed in accordance with their normal distribution by an independent t-test.

Micrococcal Nuclease Sensitivity

MNase sensitivity was examined essentially as described by Chandrasekharan et al. (2009). NIH3T3 cells grown to near confluence were harvested and suspended in ice-cold RSB (10 mM HEPES-NaOH, pH 7.4, 15 mM NaCl, and 1.5 mM $MgCl_2$) containing 1% Triton X-100 and protease inhibitor cocktail. The cells were disrupted using a Dounce homogenizer. Nuclei were collected by centrifugation and washed twice with buffer B (15 mM HEPES-NaOH, pH 7.4, 15 mM NaCl, 60 mM KCl, 0.34 M sucrose, 0.5 mM spermine, 1 mM dithiothreitol (DTT), and protease inhibitor cocktail). The nuclear pellet was resuspended in 10 volumes of storage buffer (20 mM Tris-HCl, pH 7.5, 0.1 mM EDTA, 10% glycerol, 100 mM KCl, 1 mM DTT, protease inhibitor cocktail, and 5 mM N-ethylmaleimide) and stored until use. The number of nuclei was determined by measuring the optical density at 260 nm using an aliquot resuspended in 1 N NaOH. In MNase digestion

buffer (10 mM Tris-HCl, pH 8.0, 50 mM NaCl, 5 mM KCl, and 0.2 mM EDTA) containing 2 mM $CaCl_2$, nuclei were digested by MNase (Takara) at a concentration of 10, 30, 60, and 90 U/ml for 10 min at 37 °C. The digestion was terminated by adding stop buffer (50 mM Tris-HCl (pH 8.8), 20 mM EDTA, and 0.5% SDS) and treated with 2 mg/ml proteinase K (Roche) for 1 h at 42 °C. The DNA was purified by phenol-chloroform extraction and digestion with 5 µg/ml RNase (30 min at 37°C, Nakalai Tesque), followed by a second phenol-chloroform extraction. Equal amounts of DNA (300 ng/lane) were analyzed by 2.0% agarose gel electrophoresis and stained with ethidium bromide for visualization.

Measurement of the Levels of Histone H3K9me3

The levels of histone H3K9me3 were measured using the EpiQuick global H3K9me3 quantification kit following the manufacturer's protocol (Epigentek). Briefly, after the isolation of nuclei from NIH3T3 cells, histones were prepared by acid extraction. The histone fractions were then spotted on wells coated with anti-H3K9me3 antibodies by incubation at RT for 60 min. The amount of H3K9me3 was quantified using the microplate reader via a colorimetric reaction at a wavelength of 450 nm. The experiment was repeated three times, and the mean value was acquired. The data were analyzed by an independent t-test. For the control, active and inactive chromatin fractions were prepared essentially as described by Fierz et al. (2011) and Tachiwana et al. (2010). Nuclei were isolated from NIH3T3 cells as described previously for the MNase sensitivity experiments. In the presence of 1 mM $CaCl_2$, nuclei were digested in MNase digestion buffer with 12 x 10^{-2} U/µl MNase for 12 min at 37 °C. The digestion was stopped by the addition of 10 mM EDTA, and the sample was centrifuged at 10,000 g for 10 min at 4 °C. The supernatant (S1) was collected, and the pellet was suspended in 10 mM EDTA, pH 8.0/150 mM NaCl solution. The sample was again centrifuged at 20,000 g for 10 min, and the supernatant (S2) was collected. The combined

fractions of S1 and S2 were used as an active chromatin fraction. The pellet was extracted with 0.4 N H2SO4, followed by TCA precipitation, and was used as an inactive chromatin fraction.

H3K9me3 Immunostaining of NIH3T3 Cells

NIH3T3 cells were washed once with TBS (20 mM Tris-HCl, pH 7.4, 150 mM NaCl, 2 mM KCl) for 10 min, and fixed with 80% ethanol for 15 min at RT. Cells were permeabilized with TBS containing 1% Triton X-100 for 10 min and blocked with 3% BSA in PBS for 10 min, followed by an incubation overnight at 4 °C with the primary antibodies rabbit anti-TH2B (1:200) and mouse anti-H3K9me3 (1:200). Cells were then incubated with the secondary antibodies Alexa Fluor 488 goat anti-rabbit IgG (1:300) and Alexa Fluor 546 goat anti-mouse IgG (1:300; Invitrogen). After washing, cells were incubated with TO-PRO-3 (1:1,000; Invitrogen) for 10 min at RT, washed with H2O, and mounted in ProLong Gold (Invitrogen). Samples were analyzed using a ZEISS LSM 510 confocal microscope.

2.3 RESULTS

2.3.1 Overexpressed TH2A/TH2B induce an open chromatin structure in NIH3T3 cells

To understand the mechanism by which TH2A and TH2B regulate chromatin structure, the DNase I sensitivity of nucleosomes containing TH2A/TH2B was compared to those containing canonical histones. NIH3T3 cell pool expressing TH2A/TH2B or H2A/H2B at a relatively high level were generated by the selection of neo^r cells after infection with a retrovirus expressing both TH2A/TH2B or H2A/H2B and the neo^r gene. In these NIH3T3 cells, the expression levels of TH2A and TH2B relative to endogenous H2A and H2B were 32% and 33%, respectively, and most of the TH2A/TH2B was deposited into chromatin (Fig. 2.1). The nuclei from NIH3T3 cells expressing TH2A, TH2B, and P-Npm exhibited higher DNase I sensitivity than those from cells overexpressing canonical histones (Fig. 2.2).

There was no difference in the micrococcal nuclease (MNase) sensitivity of the nuclei from those two cell pools overexpressing TH2A/TH2B or H2A/H2B (Fig. 2.3). TH2A/TH2B also did not affect the level of histone H3K9me3 (Fig. 2.4 and 2.5). Overall these results suggest that the presence of TH2A/TH2B induces a more open chromatin structure.

2.3.2 Defects in the deposition of TNP2 on chromatin in Th2a-/-Th2b-/- spermatids

During spermiogenesis, histones are replaced by transition nuclear proteins (TNP1 and TNP2), which are then replaced by protamines (Gaucher et al., 2010). The TNP2 immunostaining signal in mutant spermatids lacking TH2A/TH2B decreased substantially compared with that of the wild-type control (Fig. 2.6A). An abnormal nuclear morphology was evident in the mutant spermatids (Fig. 2.6B), although the level of Tnp2 mRNA in mutant and wild-type testes was similar (Fig. 2.7).

The levels of TNP2 and protamine 2 in mutant spermatid extracts were lower than those in the controls (Fig. 2.6C). When spermatid whole extracts were separated into chromatin and non-chromatin fractions, TNP2 and protamine 2 were predominantly recovered in the chromatin fraction and their levels in the mutant chromatin fraction were lower than those in the wild-type chromatin fraction, suggesting a defect in the chromatin incorporation of TNP2. Because there were no differences in the mRNA levels of several genes (Prm1, FoxJ1, Ube2a, Rnf12, and Tpap) between wild-type and mutant spermatids with haploid genomes (Fig. 2.7), the defect in histone replacement may have been due to an abnormality in chromatin structure rather than a decrease in haploid genome expression. In addition, there was moderate differential expression in a few dozen genes in spermatocytes of mutant and wild-type testes (data not shown), suggesting that it was unlikely that the loss of Th2a and Th2b genes in spermatogonial stem cells caused these defects in spermatogenesis. The results of western blot analysis of round and elongating spermatid extracts indicated that the H2A level was similar between the spermatids of wild-type and mutant mice, while the H2B level was higher in mutant spermatids than in the control spermatids (Fig. 2.8), suggesting the presence of a feedback mechanism.

2.4 DISCUSSION

Open chromatin is a hallmark of ESCs and iPSCs, in which the overall genome is hyperactive and the levels of heterochromatin are reduced compared with differentiated cells (Efroni et al., 2008). The open chromatin state in ESCs is maintained by multiple chromatin remodeling factors, including Chd1 and the TIP60-p400 complex (Gaspar-Maia et al., 2009; Fazzio et al., 2008). Reduction of the Chd1 level in ESCs increased the amount of heterochromatin, whereas expression of TH2A/TH2B did not affect the level of H3K9me3, a typical marker of heterochromatin. These results suggest that TH2A/TH2B contribute to the reprogramming of somatic cells by inducing transcriptionally active open chromatin, whereas Chd1 contributes to the maintenance of an established open chromatin state in ESCs by suppressing heterochromatin formation.

In spermatogenesis, it is reported that TH2B levels in spermatocytes and spermatids are approximately two-fold higher than the H2B level (Lu et al., 2009). However, the H2A levels were not significantly different in the mutant cells. We speculate that the loss of TH2A/TH2B blocks the replacement of histones during spermiogenesis Recently, Montellier et al. (2013) reported that mutant mice lacking TH2B expression exhibit no defect during spermiogenesis, indicating that a loss of TH2B alone is not sufficient to disturb histone replacement. Thus, loss of both TH2A and TH2B may be necessary to impair histone replacement and the normal release of cohesion at interkinesis. However, the possibility that such defects are due to a decrease in the total histone level cannot be excluded. In the mutant testis, the lack of TH2B was compensated by over-expression of H2B, whereas overexpression of H2A was not observed. Thus, the total amount of histones in the mutant cells was lower than that in the wild-type cells. Multiple mechanisms may act in combination to destabilize the nucleosome and replace the histones. Hyperacetylation of canonical histones during spermatogenesis, especially H4, and multiple histone variants are thought to

weaken DNA–histone octamers and nucleosome–nucleosome interactions (Govin et al., 2007; Gaucher et al., 2010). Nucleosomes containing hyperacetylated histones are thought to be more prone to displacement by protamines (Oliva et al., 1987). These previous reports are consistent with the observations that TH2A/TH2B, which induce an open chromatin structure, are required for the replacement of histones by TNPs .

CHAPTER 3. THE ROLE OF HUMAN HISTONE VARIANTS TH2A AND TH2B IN REPROGRAMMING

3.1 RESEARCH PURPOSE

Human TH2A and TH2B have high homology with mouse TH2AandTH2B respectively. Human TH2A and TH2B shared the same promoter as mouse TH2A and TH2B. Compared to canonical histone H2A and H2B, TH2A and TH2B differ at C-terminal and N-terminal respectively (Figure 4.1). TH2B is highly expressed during human spermatogenesis (Zalensky et al. 2002) and forms unstable octamer, as demonstrated in mouse (Li et al., 2005; Shinagawa et al., 2014). Histone chaperone NPM2 is also highly enriched in oocyte (Yan et al., 2013) and humanNPM2 has 66% identity with mouse NPM2. In the case of mice, co-expression of phosphorylation-mimic form of Npm2 enhanced the reprogramming efficiency in combination with TH2A, TH2B, and OSKM (Shinagawa et al., 2014).Therefore human TH2A, TH2B, and phosphorylation-mimic form of NPM2 (P-NPM2)may also have positive effects on reprogramming of human cells.

My purpose is testing whether induction of human TH2A, TH2B, and P-NPM2 can enhance reprogramming in two different primary cell types (human umbilical endothelial vein cells and adult human dermal fibroblasts). Another aspect is characterization of iPSCs generated by OSKM and TH2A, TH2B, P-NPM2 by genome wide expression profile and teratoma formation capacity compared to iPSCs generated by OSKM.

3.2 MATERIALS AND METHODS

Plasmid Construction

TH2A (*HIST1H2AA*, NM_170745.3) and *TH2B* (*HIST1H2BA*, NM_170610.2) were amplified from genomic DNA by PCR and inserted into pLenti6.3 vector. Primer sequences for generating plasmid were listed in Table 3.1

Expressions of TH2A and TH2B in adult human dermal fibroblasts (HDFs) infected with those expression vectors were confirmed by Western blot with anti-TH2A and anti-TH2B antibodies (Shinagawa et al., 2014). Prediction of phosphorylation sites of NPM2 was carried out by using KinasePhos (Huang et al., 2005). Phosphorylation-mimic nucleoplasmin P-NPM was custom synthesized from Operon Biotechnologies Inc. (Tokyo, Japan), in which 10 putative phosphorylated amino acid residues (4, 5, 7, 8, 9, 86, 99, 191, 196, and 204) were substituted to Asp.

Generation and Maintenance of Human iPSCs

Adult human dermal fibroblasts (HDFs) and human umbilical vein endothelial cells (HUVECs) were purchased from LifeTechnologies (Waltham, MA). HDFs and HUVECs were passaged once and stored at -80°C before use. HDFs were maintained in fibroblast medium (Medium M106with LSGS supplement, Life Technologies). HUVECs were maintained in EGM-2 BulletKit (LifeTechnologies). Human neonatal dermal fibroblasts (CC-2509) we obtained from Lonza-Life Technologies, and maintained in FGM-2 BulletKit fibroblast medium(Life Technologies).

Lentivirus system was used to generate induced pluripotent stem cells. Plasmids pSIN4-EF2-O2S and pSIN4-CMV-K2M (Yu et al., 2009) were obtained from Addgene

(Cambridge, MA) (#21162 and #21164). Four millions of 293T cells were plated in 10 cm dish 1 day before transfection. Lentiviral vectors were packaged with a pLP1, pLP2, and pLP/VSVG (Life Technologies) or psPAX2, pMD2.G (Addgene) for pLenti 6.3 and pSIN4 respectively. Virus containing supernatant was concentrated by LentiX concentrator (Clontech,Mountain View, CA), finally suspended in 1/10 volume of medium. Fifty thousand HDFs and HUVECs were infected with a mixture of each 50 µl lentiviral vector solution for 24 hours 3 hours, respectively. Empty vector viral solution was used to adjust the volume. Virus containing medium was change to fibroblast medium or EGM medium and cells were cultured for 48 hours. Infected cells were passage 1/4into 6-well plate containing mitomycin C treated MEFs as feeders. Cells were maintained in human ES medium (20% Knockout serum replacement [Life Technologies], 10 ng/ml bFGF, 1 mM glutamine, 100 µM non-essential amino acid, 100 µM 2-mercaptoethanol, 50 unit/ml streptomycin/penicillin in Knockout DMEM).

Individual colonies were picked up and expanded. Cells were passaged every 3 days by CTK solution (containing 0.1 mg/ml collagenase type IV (Sigma) and 0.025% trypsin (Life Technologies), 1 µM $CaCl_2$ and 20% Knockout serum replacement in water).

In some case, adult HDFs were infected with virus to express BAN or empty vector for 24 hours. Infected cells were then cultured in fibroblast medium and passaged once. After 5 days infection, cells were infected with virus to express OSKM as described.

Cell proliferation assay

At day 0, adult human fibroblasts were seeded at indicated number. Same amount of virus-containing medium as mentioned above were used to infect cells for 24 hours. Infected

cells were counted at day 5 and day 8 post infection by Countess II Automated Cell Counter (Life Technologies).

Immunofluorescence Staining

Live cell staining was performed with anti-SSEA4 (BD Biosciences) and anti-TRA-1-60 antibodies (BD Biosciences). First antibody was diluted 1/300, second antibody was diluted 1/500 in cell culture medium, mixed and stood for 2 minutes. Cells were incubated with diluted antibody for 45 minutes at 37°C. Antibodies were removed and washed twice with human ES medium. Images were taken immediately after staining.

For staining ofOCT4 and NANOG, cells were fixed by 2% paraformaldehyde in PBS, permeabilized with 1% Triton-X100 in PBS, then incubated with anti-OCT4 (Santa Cruz) and anti-NANOG (Abcam) antibodies diluted in 1% BSA in PBS for 2 hours at room temperature. Secondary antibodies (Life Technologies) were diluted 1/1000 in 1% BSA in PBS for 2 hours at room temperature. Nuclei were stained by Hoechst 33342. Slides were mounted in Prolong Gold (Invitrogen). Images were taken by ZEISS LSM 510 confocal microscope.

For immunohistochemistry, tissues were fixed in 4% PFA in PBS at 4°C for 3 hours, embedded in paraffin, and sectioned into 5 µm thickness. Following antibodies were used: anti-SMA, anti-TUJ1, anti-AFP (Invitrogen).

Alkaline Phosphatase Staining

Alkaline phosphatase staining was performed according to the instruction of Leukocyte Alkaline Phosphatase Kit (Sigma-Aldrich, St. Louis, MO). Cells were fixed with 2% paraformaldehyde in PBS for 1-2 minutes. Fixed cells were incubated in alkaline staining solution for 15 minutes at room temperature in dark.

In vitro differentiation

iPSCs were dissociated with CTK solution as described above. Confluent iPSCs in one well of 12-well-plate were collected and suspended in 1 ml of human ES medium without bFGF. Cells were transferred into 12-well non-adherent plate and culture for 3 days to form embryoid bodies. Embryoid bodies were transferred into adherent plate for spontaneous differentiation. Six days after transfer, differentiated cells were fixed and stained with antibodies against SMA, TUJ1, and AFP (Invitrogen).

Teratoma Formation

Teratoma formation was performed as described by Gropp et al. (2012). iPSCs were dissociated into single cells by accutase and pass through a 70 μm cell strainer. $5x10^5$ iPSCs were mixed with $5x10^5$ mitomycinC treated MEFs and suspended in 50 μl of PBS. For negative control, $1x10^6$ mitomycinC treated MEFs were used. Cells were combined with 50 μl Matrigel (BDBiosciences, San Jose, CA) immediately before transplantation and injected subcutaneously into the dorsal flanks of NOD/ShiJic-*scid*Jcl (NOD/SCID) mice (Clea Japan, Tokyo, Japan).

Teratomas were dissected 6-9 weeks after injection.

To analyze the area occupied by epithelial-like structures, images of nonconsecutive sections (n = 10-12) of each teratoma were acquired and processed by Zeiss Axio Vision 4.8.2. For each teratoma, the areas of 100 to 120 epithelial-like structures were randomly selected and their sizes were measured.

Hematoxylin and eosin staining

Tissues were fixed in 4% PFA at 4°C for 3 hours. After fixation, tissues were dehydrated by ethanol and butanol, finally were embedded in paraffin. Fixed tissues were sectioned into 5 μm thickness. Sections were rehydrated and stained with Mayer's hematoxylin (Wako, Tokyo, Japan) for 10 minutes, then rinsed with tap water for 15 minutes, finally stained with 1% eosin for 15 minutes. Stained sections were dehydrated and mounted in Entellanneu (Merck).

Quantitative RT-PCR (qRT-PCR)

RNAs were extracted by Qiagen Rneasy Minikit (Qiagen). Total RNA (100 ng) was used for qRT-PCR reaction by RNA direct SYBR Green realtime PCR master mix (Toyobo, Osaka, Japan). Sequence specific primers were listed in Table 3.2.

Microarray analysis

Total RNAs were extracted by ISOGEN (Nippongene) from 3 independent OSKM iPSC clones and 3 independent OSKMBAN iPSC clones. Total RNAs were amplified by

Ambion WT Expression Kit (Life Technologies) and hybridized to Human Gene 1.0 ST Array (Affymetrix).

Data processing

Microarray data was processed with R package Oligo (http://www.r-project.org). RMA algorithm was used to normalize all the expression data at the same time. GEO dataset for human fibroblasts and human embryonic stem cells were retrieved from GSE23034 (Ohi et al., 2011). GSEA (Gene Set Enrichment Analysis) (Subramanian et al., 2005) was performed by default setting, except that the minimum size and maximum of gene set were set to 30 and 400 respectively. For GSEA of naïve stem cells, four fold up- or down-regulated transcripts by naïve stem cells compared to primed stem cells (Theunissen et al., 2014) were used for up- or down-regulated naïve stem cells transcripts gene sets. GSEA analysis were performed by default setting.

Table 3.1 Specific primers for qRT-PCR

	Forward (5'-3')	Reverse (5'-3')
GAPDH	CCCCAGCAAGAGCACAAGAG	AGGGGAGATTCAGTGTGGTG
Exogenous SOX2	GGCCATTAACGGCACACTG	TGCTTCTAGCCAGGCACAAT
Exogenous c-MYC	GGGGACGTGGTTTTCCTTTG	TTCTCCTCCTCGTCGCAGTA
NANOG	CAATGGTGTGACGCAGAAGG	GAAGGTTCCCAGTCGGGTTC
Endogenous OCT4	TTGGGAACACAAAGGGTGGG	ACTGTGTCCCAGGCTTCTTTA
GDF3	ATCCCTGTCCCCAAGCTTTC	AACCCAGGTCCCGGAAGTTA

Table 3.2. Primers for plasmid construction

Name	Sequence
SpeI-NPM-F	ATCGACTAGTCCACCATGAATCTCGATG ACGCCG
XhoI-NPM-rev	AATGCTCGAG TCATTTCTTGAATCCTGGCTTC
H2AA-SpeI-F	AGTAACTAGTCCACCATGTCTGGACGAGGGAAG
H2AA-XhoI-R	AGTACTCGAGTTACTTGCTTTGGGCTTT
H2BA-SpeI-F	AGTAACTAGTCACCATGCCGGAGGT
H2BA-XhoI-R	AGCTCTCGAGTTACTTGGAGCTGGTGTACT

3.3 RESULTS

3.3.1 Human TH2A, TH2B, and NPM2 enhance the reprogramming

To determine whether human TH2A, TH2B and NPM2 (BAN) have a role in reprogramming, I coexpress OCT4, SOX2, KLF4, and c-MYC with BAN in human primary cells.

Human umbilical vein endothelial cells (HUVECs) are reported as easily reprogrammed cells and its source is abundant and noninvasive. Thus I first examined whether efficiency of OSKM-induced iPSC generation is affected by overexpression ofTH2B, TH2A, and phosphorylation-mimic form of NPM2 in HUVECs. To detect reprogrammed cells, live cells were stained with anti-TRA-1-60 antibody (Chan et al., 2009). After 11 days post infection, BAN enhanced the generation of OSKM-induced TRA-1-60 positive colonies 7.6-fold (Fig. 3.2A). At day 16, higher number of alkaline phosphatase positive colonies were observed in cells induced BAN and OSKM compared to OSKM alone (Fig. 3.2B). To further confirm the data, I perform staining of SSEA4, another marker for reprogrammed cells (Chan et al., 2009). SSEA4 positive colony number was also increased by the addition of BAN (Fig. 3.2C). As for application in regenerative medicine, human adult dermal fibroblasts (HDFs) are better sources, which can be collected from people with an acceptable damage. BAN also enhance the reprogramming of HDFs by2.2 fold (Fig. 3.3A). When neonatal human dermal fibroblasts (neonatal HDFs) were used, BAN also enhanced the reprogramming by 2.2-fold (Fig. 3.3B). I also tested whether prolonged BAN expression modulates reprogramming efficiency of adult HDFs, because adult HDFs are better cell source compared to neonatal HDFs for application purpose. Cells were infected with virus to express BAN or empty vector for 24 hours. Infected cells were cultured in fibroblast medium and passaged once. After 5 days infection, cells were infected with virus to express OSKM. At day 16 after

OSKM infection, the number of SSEA4-positive colony was enhanced 10.7-fold by prolonged BAN expression (Figure 3.4). This observation suggests that much amount of histone variant TH2A/TH2B need time to be incooporated into chromatin prior to OSKM expression

Colonies generated by OSKMBAN from HDFs expressed NANOG and OCT4 with the typical homogenous nuclear staining pattern and showed flat morphology similar to human ESCs or iPSCs (Fig. 3.5). Of note, overexpression of BAN did not affect the proliferation rate of human adult dermal fibroblasts (Figure 3.6).

Taken together, BAN can enhance the reprogramming process in human cells.

3.3.2 Differentiation capacity of OSKMBAN iPSCs

To investigate the pluripotency of human iPSCs generated by OSKMBAN, I performed the *in vitro* and *in vivo* differentiation assay. After 9 days of culture in differentiation medium, clones of OSKMBAN iPSCs expressed the markers for three germ layers: beta-III tubulin (TUJ1) for ectoderm, smooth muscle actin (SMA) for mesoderm, and alpha-fetoprotein (AFP) for endoderm (Fig. 3.7). Subcutaneous injection of iPSC clones into SCID/NOD mice generate teratomas5-9 weeks later (Fig. 3.8). Hematoxylin and eosin staining of teratomas showed morphology of chondrocytes (mesoderm), neural rosette (ectoderm), and epithelial-like structure (endoderm) (Fig. 3.9A), and they were further confirmed by immunostaining of the three germ layer markers (Fig. 3.9B). Teratomas derived from OSKMBAN iPSCs contain more diverse structure and high density of epithelium-like area than that from OSKM iPSCs (Fig. 3.10).These results suggest that OSKMBAN iPSCs have a better differentiation capacity than OSKM iPSCs *in vivo*.

3.4.3 Gene expression profiles of OSKMBAN iPSCs

To understand how TH2A, TH2B and NPM2 affect the characteristic of OSKMBAN iPSCs at molecular level, whole transcript expression analysis was performed. Three individual clones of OSKMBAN iPSCs and three individual clones of OSKM iPSCs as control were used for study of whole genome expression by Human Gene 1.0 ST array. Human ESCs and fibroblasts data of the same platform (Ohi et al., 2011) were used for comparison. OSKMBAN iPSC clones are clustered with OSKM iPSC clones in the same group with human embryonic stem cells, indicating that OSKMBAN iPSCs possess similar properties with human ESCs at gene expression level (Fig. 3.11). The pluripotent group containing human ESCs, OSKM iPSCs and OSKMBAN iPSCs is distant from human fibroblasts group. The scatter plot of average gene expression levels of three OSKMBAN iPSC clones and fibroblasts indicates that OSKMBAN iPSCs are distinct from fibroblasts (Fig. 3.12). The pluripotent markers (OCT4, SOX2, NANOG, ZFP42 and GDF3) shown in red dots are highly expressed in OSKMBAN iPSCs than fibroblasts. Expression patterns of OSKMBAN iPSCs show a higher similarity to OSKM-induced iPSCs (r^2=0.99) than that of human ESCs (r^2=0.96). To confirm the data, expression levels of endogenous OCT4, NANOG, and GDF3 were measured by qRT-PCR (Fig. 3.13). These pluripotent genes showed high expression in OSKMBAN iPSCs and OSKM iPSCs compared to human fibroblasts.

One of the characteristics of pluripotent stem cells is the suppression of retroviral and lentiviral transgenes. Expression levels of c-MYC and SOX2 from lentiviral vector in iPSC clones were compared (Fig. 3.14).Exogenous c-MYC expression driven by CMV promoter was significantly downregulated in all iPSC clones. On the other hand, SOX2 was persistently expressed under the control ofEF1 promoter, suggesting that EF1 promoter is

relatively resistant to suppression in pluripotent cells in agreement with previous study (Xia et al., 2007).

To evaluate the differences of expression profile between OSKMBAN and OSKM iPSCs, I performed the gene set enrichment analysis (GSEA) (Subramanian et al., 2005). Upregulated genes in OSKMBAN iPSCs were involved in pathways including glycolysis and JAK-STAT pathway (Fig. 3.15). Recently human ESCs andiPSCs which appear to be similar to naïve mouse ESCs have been reported (Gafni et al., 2013; Takashima et al., 2014; Ware et al., 2014; Theunissen et al., 2014). These naïve pluripotent stem cells develop high grade teratoma and the same property was observed in OSKMBAN iPSCs. Thus I perform the GSEA comparing up or down regulated genes in OSKMBAN iPSCs to OSKM iPSCs and up- or down-regulated genes in human naïve ESCs to primed ESCs (Theunissen et al., 2014). Transcripts which show more than4 fold up- or down-regulation were used for analysis. GSEA analysis revealed that upregulated genes in OSKMBAN iPSCs are significantly enriched in the upregulated gene set of naïve ESCs. On the other hand, genes up-regulated in OSKM iPSCs are significantly enriched in the gene set down-regulated in naïve stem cells(Fig. 3.16). These data suggest that TH2A, TH2B, and NPM2 may regulate genes which involve in naïve state of pluripotency.

3.4 DISCUSSION

In this study, human TH2A, TH2B and P-NPM2 are shown to enhance reprogramming by Yamanaka 4 factors and resulting iPSCs exhibit high differentiation capacity *in vitro* and *in vivo*. Hematoxylin and eosin staining analysis confirmed that after transplantation into NOD/SCID mice, human OSKMBAN iPSCs formed well-differentiated teratomas, which consisted of all three germ layers, including chondrocytes (mesoderm), neural rosette (ectoderm), and epithelial-like structure (endoderm). These data suggests that OSKMBAN iPSCs can readily differentiate into other cell phenotypes. It has been reported that cell origin of iPSCs can affect the range of differentiation due to aberrant DNA methylation on genome (Lister et al., 2011; Ohi et al., 2011; Bar-nur et al., 2011). TH2A, TH2B, and P-NPM2 may have an influence on DNA demethylation process by forming open chromatin structure (Shinagawa et al., 2014).

Compared to canonical histones, histone variants are only different in several amino acids which resulting in different functions. One of the most well studied histone variants is histone H3.3, which is highly conserved in metazoan. Histone H3.3 differs from canonical histone H3.1/H3.2 by only four to five amino acids. H3.3 is associated with active transcribed genes by recruiting histone modifications associated with gene activation such as K4, K36 and K79 methylation and K9 and K14 acetylation, which are hallmarks of open chromatin structure. Moreover histone H3.3 form unstable nucleosomes and promote gene activation among with histone H2A.Z (Jang et al., 2015). Since TH2A and TH2B are also differ by several amino acids compared to canonical histone H2A and H2B, TH2A and TH2B have a positive role in reprogramming. There observations suggest that each amino acid in the histone structure is important and specify the role of histone.

The tails of histones are key players for modulating chromatin activity. Compared to H2A and H2B, TH2A and TH2B are differ by the C-terminal and N-terminal respectively.

Histone H2A C-terminal tail regulates chromatin structure and dynamics (Vogler et al., 2010). H2A C-terminal tail stabilizes the nucleosome core particle, as well as mediates protein-protein interaction with chromatin remodelers and linker histone H1. Histone H2B N-terminal tail has been reported to linked to nucleosome stability (Iwasaki et al., 2013). Moreover, most of histone posttranslational modifications exist in the N-terminal tail (Parra et al., 2006). Multiple lysine acetylation residues have been reported in the N-terminal tail of H2B (K6, K11, K16, K17, K21 and K22). The acetylation in this domain is required for transcriptional activation in gene-specific context. Taken together, the difference in C-terminal and N-terminal of TH2A and TH2B compared to H2A and H2B may result in a more striking distinct function. TH2A and TH2B tails may recruit specific chromatin remodeling proteins, which can act to recruit other histone H3/H4 modifications. Coimmunoprecipitation experiments to identify proteins which interact with TH2A/TH2B tails may shed light into the function of these histone variants.

Since histone modifications play a vital role in the function of histones, TH2A and TH2B posttranslational modifications may also have critical role. In the reprogramming process triggered by Yamanaka four factors, starting materials are somatic cells. On the other hand, TH2A and TH2B are specifically expressed in later stages of spermatogenesis and mature oocyte. Some factors which are responsible for TH2A and TH2B posttranslational modifications may not exist in somatic cells, therefore in the somatic cell context, TH2A and TH2B may not get sufficient modifications. To explore these possibilities, TH2A and TH2B posttranslational modifications should be identified by mass spectrometry in spermatogenesis or ideally in mature oocytes.

During the developmental process, the zygote, which is totipotent, gradually lose its developmental capacity and commits to cell fate decisions. This process is driven by cross-antagonistic transcription factors. The simplest model is that a transcription factor promote a

specific cell fate by repress an alternative different pattern. Although cell identity is stable, it can be altered by ectopic expression of four transcription factors OSKM. The expression of these four factors destabilize the somatic gene network and establish the ES-like phenotype. In addition to modifying the transcriptional network, overexpression of four factors OSKM during reprogramming induce large scale chromatin remodeling, which finally lead to an open chromatin structure similar to ESCs. Upon binding to their target sites, OSK enable the binding of other transcription factors and/or recruit histone modifiers. In addition, the binding of these OSK can induce locus-specific DNA demethylation. Therefore in this model, the chromatin change is not involved in the reprogramming process, but rather reflects the successful establishment of pluripotent state.

In contrast to this viewpoint, recent studies suggest a more important role of chromatin in early stage of reprogramming. Soufi et al. (2012) showed that repressive histone modifications and heterochromatin block the initial binding of OSK in early reprogramming stage. Moreover, in trans-differentiation process, repressive chromatin is also responsible for the failure of gene network reactivation (Cahan et al., 2014; Morris et al., 2014). Especially in reprogramming, H3K9me2/me3 histone modifications, which are repressive markers, and DNA 5mC modification are reported to be a barrier (Mikkelsen et al., 2008; Lister et al., 2011; Chen et al., 2013; Sridharan et al., 2013). Taken together, these observations suggest that an open chromatin structure is an optimal starting point for transcription factors to access. In chapter I of this study, histone TH2A/TH2B induce an open chromatin structure, which would explain their positive effect in reprogramming.

Indeed many chromatin remodeling factors are important in somatic cell reprogramming. For example, the SWI/SNF family, in which esBAF (Brm/Brg associated factor) and Ino80 (Inositol requiring 80) promote the binding and activity of OSKM during reprogramming (Singhal et al., 2010). In contrast to the remodeling complexes which induce

an open chromatin structure, the NuRD (Nucleosome remodeling deacetylase) complex, in which Mbd3 is a core subunit contains histone deacetylase activity. Depletion of Mbd3 significantly enhance the reprogramming efficiency (Rais et al., 2013) through facilitate the re-activation of OSKM targets.

In case of histone variants, histone H3.3 maintains an open chromatin configuration by counteract with linker histone H1-mediated chromatin compaction (Braunschweig et al., 2009). In somatic cell nuclear transfer, histone H3.3 is deposited into somatic donor cell, depletion of H3.3 cause failure in reprogramming (Jullien et al., 2012). However, the role of H3.3 in reprogramming by OSKM has not been studied. In comparison with TH2A, TH2B and H3.3, marco H2A, which possess a unique macro domain and distinct from other canonical histones, is shown to associated with heterochromatin. In ESCs, the level of marco H2A is significantly lower than somatic cells, and increasing during the differentiation (Creppe et al., 2012). Macro H2A has been shown to be a barrier in reprogramming by OSKM. In the absence of macro H2A, iPSC reprogramming efficiency is up 25 fold (Pasque et al., 2012). It would be an interesting idea to test the combination of these chromatin modifiers and histone variants in reprogramming, because *in vivo* and in the reprogramming by somatic cell nuclear transfer, all of these factors seem to work in concert.

In earlier report (Shinagawa et al., 2014), we investigated the role of mouse TH2A, TH2B and P-Npm2 in reprogramming of MEFs. TH2A, TH2B and P-Npm2 enhanced OSKM dependent iPSC generation by produced iPSCs with Oct4 and Klf4. The enhancement of TH2A, TH2B and P-Npm2 in mouse system is more than 20 folds, which is significantly higher than human system. One of the reason is that the starting materials are different in term of developmental age. Mouse embryonic fibroblasts are collected at E13.5, while human cell source is later in development (HUVECs, adult and neonatal dermal fibroblasts). During

the development, the genome and epigenome are further modified, which could lead to a difficulty in erasing and reestablishment.

iPSCs have a memory and they tend to differentiate to origin cell type. During the reprogramming process, the epigenome of somatic cells is erased and established again. In contrast to high level of DNA methylation in somatic cells, DNA methylation in the naïve stem cells are much lower. The relationship between a faithful transcriptome and DNA methylome are demonstrated recently (Ma et al., 2014) by using the same starting material for both reprogramming methods: transcription factors induced and somatic cell nuclear transfer. Interestingly, a strong correlation between incomplete reactivation of gene expression during reprogramming and high promoter methylation in iPSCs. These observation suggests DNA methylation might be responsible for the memory of iPSCs, which cause them to easily differentiate into original cell type.

In theory, iPSCs are ideal for regenerative medicine and disease modelling. Compared to ESCs, iPSCs can be derived from patients, therefore their uses would not be hindered by ethical issues. However, many groups have reported that in the mouse system, iPSCs are not uniform in their differentiation capacity compared to ESCs. Some iPSC lines can differentiate into three germ layers *in vitro* but fail to contribute to the embryo. Tetraploid complementation is a more stringent assay compared to traditional chimera assay, in which some iPSC lines can contribute to chimeras but fail to generate embryo in tetraploid assay. These observations suggest a significant variation in the quality of iPSCs in mice. Furthermore, many mouse rigorous functional assays such as chimera contribution, tetraploid complementation are not applicable with human iPSCs. In this study, iPSCs are induced from adult dermal fibroblasts, therefore epithelial-like structures, which are representive of endodermal lineage, are a good indicator of the differentiated capacity of iPSCs. Moreover, Ware et al., 2014 showed the naïve stem cells have a robust contribution to endodermal

lineage compared to prime stem cells. In order to assess the naïve stem cells *in vivo*, these cells should be injected into ICM or early blastocysts and monitor the contribution to the embryo. However, regarding the ethic and scarcity of human embryos, teratoma assay is still a gold standard in current situation. Since one of human iPSCs application aspect is drug screening. In this context, iPSCs need to be differentiated into desired cell types *in vitro*. A high quality iPSCs should be easily differentiated into any lineages with high efficiency. *In vitro* differentiation assay into specific cell type should be used to assess the capacity of human iPSCs generated by OSKMBAN.

Generally exogenous gene expression is desired to be silenced in human ESC/iPSCs. Exogenous SOX2 expression driven by EF1 promoter is still retained. On the other hand, exogenous c-MYC expression driven by CMV promoter is suppressed in spite of delivering by the lentiviral vector. In agreement with these observations, Xia et al. (2007) reported that expression of gene delivered by lentiviral vector in human ESCs is depend on promoter. CMV promoter is highly suppressed while EF1 promoter is not affected in human embryonic stem cells. Therefore human OSKMBAN iPSCs are similar to human ESCs in the context of transgene promoter silencing, which exhibit high suppression of CMV promoter.

The effect of BAN is depend on the cell type of origin. BAN can enhance the number of TRA-1-60 and SSEA-4 positive colony number in HUVECs about 8 fold and 3.5 fold respectively. On the other hand, the degree of enhancement for adult dermal fibroblast is approximately 2.5 fold. It is reported that HUVECs can be reprogrammed with high efficiency and faster kinetic compared to adult fibroblast (Panopoulos et al., 2011). In agreement which Panopoulos et al., when using HUVECs, SSEA-4 positive colony can be detected as early as 10 days post infection. During the reprogramming process, chromatin is reorganized and open chromatin structure is formed. HUVECs may efficiently form open chromatin than adult fibroblasts. Therefore BAN maybe more easily incooperated into

chromatin of HUVECs than adult fibroblasts, thus the effect of BAN in reprogramming of HUVECs is more prominent compared to adult fibroblasts.

When BAN is expressed prior to OSKM induction, the efficiency of reprogramming in more augmented. This observation suggest that histone TH2A and TH2B need to be incorporated at a relative high level into the chromatin prior the present of OSKM. After several DNA replications and cell divisions, TH2A and TH2B can prepare a permissive chromatin structure which may promote the binding of OSKM into their targets site. Indeed, DNA synthesis is a pre-requisite for reprogramming by somatic cell fusion (Tsubouchi et al., 2013). One speculation is that during the DNA replication, the existing chromatin structure is disrupted and reestablished and incorporation of histone variants occur.

In mouse system, we found that TH2A and TH2B are enriched on the X chromosome compared with autosomes during the reprogramming (Shinagawa et al., 2014). Furthermore the iPSC generation using TH2A and TH2B is enhanced when using *Xist* knockout MEFs. Inoue et al. (2010) reported that the cloning efficiency of both male and female cells by somatic cell nuclear transfer is increased by *Xist* deletion. This finding suggests that changes in the chromatin structure of the X chromosome affect the reprogramming process, although the mechanism is unknown. These results suggest that the mechanism of reprogramming using TH2A and TH2B in combination with OSKM is more closely linked to reprogramming by somatic cell nuclear transfer, in addition TH2A and TH2B also play a functional role in reprogramming by somatic cell nuclear transfer. TH2A and TH2B enhanced the OSKM reprogramming in both female and male MEFs, suggesting that TH2A and TH2B action mechanism is not likely to be associated with the reactivation of inactive X chromosome. On both the X chromosome and autosomes, TH2A and TH2B are distributed uniformly, which is consistent with a recent report showing that TH2B is not enriched at specific loci in spermatocytes and spermatids (Montellier et al., 2013). Therefore TH2A and TH2B facilitate

reprogramming by changing the whole chromatin structure rather than by regulating the expression of specific genes.

Comparison between OSKM and OSKM induced iPSCs, TH2A and TH2B regulated genes are overlapped with transcript signature of naïve human ESCs. Recently many reports have shown that human pluripotent stem cells can be toggled back and forth between two states “naïve” and “prime” (Chan et al., 2013; Gafni et al., 2013; Takashima et al., 2014; Theunissen et al., 2014; Ware et al., 2014). Naïve state cells are showed to have a high cellular potency due to the genome wide low methylation levels (Takashima et al., 2014; Theunissen et al., 2014) and low expression of lineage specific genes (Theunissen et al., 2014). These naïve stem cells are closely resemble to the early blastocyst stage while the prime stem cells resemble post implantation stage. In mice, TH2A and TH2B are highly deposited into X chromosome (Shinagawa et al., 2014). However these naïve genes are not enriched in X chromosome, which indicate the activation of these genes is a secondary effect. Until now mechanisms underlie the naïve state is still unclear and how TH2A and TH2B involve in this naïve state is an interesting topic for further research.

Stella/DPPA3/PGC7 is a good marker for high quality iPSCs. Recently many groups have reported the existence of naïve stem cells, which possess high quality compared to prime stem cells. These reports differ in medium and factors used for induction of naïve stem cells, which make the mechanism lying this phenomena seems obscured. However, most of the global gene expression data indicated that Stella/DPPA3/PGC7 is upregulated in all the naïve stem cell lines compared to prime stem cells. Including current study, which TH2A and TH2B also upregulated Stella/DPPA3/PGC7, this gene may be a good marker for high quality iPSCs. Interestingly, Stella is highly expressed in oocyte and the expression gradually reduce until ICM stage. In reprogramming process by OSKM, Stella/DPPA3/PGC7 is the last gene which is only expressed by fully reprogrammed cells in the stabilization stage.

The pathway analysis categorized BAN-upregulated genes in glycolysis and gluconeogenesis. Interestingly, naïve cells favor glycolysis while differentiated cells rely on oxidation. Glycolysis provides acetyl-CoA for maintaining the histone acetylation and blocking the glycolysis forces the cells into differentiation (Panopoulos et al., 2012; Moussaieff et al., 2015). Taken together, these suggest that TH2A, TH2B, and P-NPM2 induce metabolic changes from oxidation to glycolysis, resulted in high cellular potency.

BAN-upregulated genes are also enriched in Jak-Stat signaling pathway. This pathway and pluripotency network have been well studied. Stat3 is an important protein which links the LIF-signal into the pluripotent gene network. Stat3 is a transcription factor after translocating into the nuclei. It has been reported that Klf4 is a direct target of Stat3, while many other transcription factors are regulated by Stat3 such as Zfp57, Tfcp2l1 and Gbx2. Moreover the naïve state specific genes include Klf2, Klf4, Klf5, Tbx3, Esrrb and Nr0b1 are known as transcription factors which are downstream of LIF (Ohtsuka et al., 2015). Chen et al. recently reported that reinforcement of Stat3 in human ESCs can promote them into a naïve stem cell state.

In summary, histone TH2A, TH2B and P-NPM2 enhance the reprogramming in human cells and improve the quality of iPSCs. This study indicate that addition of TH2A, TH2B and P-NPM2 in the reprogramming cocktail may be a useful tool for generating clinical grade iPSCs effectively.

There are two major methods for reprogramming a somatic nucleus: somatic cell nuclear transfer and ectopic expression of embryonic enriched transcription factors. These two methods differ in their technical difficulty, efficiency of reprogramming, kinetic of reprogramming. In this study, the use of oocyte enriched factors facilitate the reprogramming by embryonic enriched transcription factors. However, one of the most intriguing questions in

this field is the kinetic of reprogramming by oocyte is only two to three days while retaining an intact genome and result in faithful totipotent/pluripotent cells. Histone TH2A and TH2B seem to be one of those key players in oocyte reprogramming. Screening of other oocyte enriched factors may be the answer for this question.

CHAPTER 4. REFERENCES

Aksoy, I., R. Jauch, V. Eras, A.C.W. Bin, J. Chen, U. Divakar, C.K.L. Ng, P.R. Kolatkar, L.W. Stanton, 2013. Sox transcription factors require selective interactions with Oct4 and specific transactivation functions to mediate reprogramming. Stem Cells 31:2632–2646.

Ang, Y.S., S.-Y. Tsai, D.-F. Lee, J. Monk, J. Su, K. Ratnakumar, J. Ding, Y. Ge, H. Darr, B. Chang, et al, 2011. Wdr5 mediates self-renewal and reprogramming via the embryonic stem cell core transcriptional network. Cell 145:183–197.

Braunschweig, U., Hogan, G. J., Pagie, L., and van Steensel, B., 2009. Histone H1 binding is inhibited by histone variant H3.3. The EMBO journal, 28(23), 3635-3645.

Bar-Nur, O., Russ, H. A., Efrat, S., & Benvenisty, N., 2011. Epigenetic memory and preferential lineage-specific differentiation in induced pluripotent stem cells derived from human pancreatic islet beta cells. Cell stem cell 9:17-23.

Bañuelos, S., M.J. Omaetxebarria, I. Ramos, M.R. Larsen, I. Arregi, O.N. Jensen, J.M. Arizmendi, A. Prado, A. Muga, 2007. Phosphorylation of both nucleoplasmin domains is required for activation of its chromatin decondensation activity. J. Biol. Chem. 282:21213–21221.

Blaschke, K., K.T. Ebata, M.M. Karimi, J.A. Zepeda-Martínez, P. Goyal, S. Mahapatra, A. Tam, D.J. Laird, M. Hirst, A. Rao, et al, 2013. Vitamin C induces Tet-dependent DNA demethylation and a blastocyst-like state in ES cells. Nature 500:222–226.

Beddington, R. S., & Robertson, E. J., 1999. Axis development and early asymmetry in mammals. Cell 96:195-209.

Buganim, Y., D.A. Faddah, A.W. Cheng, E. Itskovich, S. Markoulaki, K. Ganz, S.L. Klemm, A. van Oudenaarden, R. Jaenisch, 2012. Single-cell expression analyses during cellular reprogramming reveal an early stochastic and a late hierarchic phase. Cell 150:1209–1222.

Brons, I.G., Smithers, L.E., Trotter, M.W., Rugg-Gunn, P., Sun, B., Chuva de Sousa, Lopes, S.M., Howlett, S.K., Clarkson, A., Ahrlund-Richter, L., Pedersen, R.A., Vallier, L., 2007. Derivation of pluripotent epiblast stem cells from mammalian embryos. Nature 448:191–195.

Bryant, J. M., Meyer-Ficca, M. L., Dang, V. M., Berger, S. L., & Meyer, R. G., 2013. Separation of spermatogenic cell types using STA-PUT velocity sedimentation. Journal of visualized experiments: JoVE 80.

Cahan, P., Li H., Morris S.A., Lummertz da Rocha E., Daley G.Q., Collins JJ.., 2014. Cell Net: network biology applied to stem cell engineering. Cell 158: 903–915.

Chan, E.M., Ratanasirintrawoot, S., Park, I.H., Manos, P.D., Loh, Y.H., Huo, H., Miller, J.D., Hartung, O., Rho, J., Ince, T.A., Daley, G.Q., Schlaeger, T.M., 2009. Live cell imaging distinguishes bona fide human iPS cells from partially reprogrammed cells. Nat. Biotechnol. 27:1033–1037.

Chandrasekharan, M.B., Huang, F., and Sun, Z.W., 2009. Ubiquitination of histone H2B regulates chromatin dynamics by enhancing nucleosome stability. Proc. Natl. Acad. Sci. USA 106:16686–16691.

Chung, Y.G., Eum, J.H., Lee, J.E., Shim, S.H., Sepilian, V., Hong, S.W., Lee, Y., Treff, N.R., Choi, Y.H., Kimbrel, E.A., Dittman, R.E., Lanza, R., Lee, D.R., 2014. Human somatic cell nuclear transfer using adult cells. Cell Stem Cell 14:777–780.

Chen, J., H. Liu, J. Liu, J. Qi, B. Wei, J. Yang, H. Liang, Y. Chen, J. Chen, Y. Wu, et al, 2012. H3K9 methylation is a barrier during somatic cell reprogramming into iPSCs. Nat Genet 45:34–42.

Cho, C., W.D. Willis, E.H. Goulding, H. Jung-Ha, Y.C. Choi, N.B. Hecht, E.M. Eddy, 2001. Haploinsufficiency of protamine-1 or -2 causes infertility in mice. Nat. Genet. 28:82–86.

Creppe, C., Janich, P., Cantariño, N., Noguera, M., Valero, V., Musulén, E., ... and Di Croce, L., 2012. MacroH2A1 regulates the balance between self-renewal and differentiation commitment in embryonic and adult stem cells. Molecular and cellular biology, 32(8), 1442-1452.

Dean, W., Santos, F., & Reik, W., 2003. Epigenetic reprogramming in early mammalian development and following somatic nuclear transfer. In Seminars in cell & developmental biology 14:93-100.

Efroni, S., Duttagupta, R., Cheng, J., Dehghani, H., Hoeppner, D.J., Dash, C., Bazett-Jones, D.P., Le Grice, S., McKay, R.D., Buetow, K.H., Gingeras, T.R., Misteli, T., and Meshorer, E., 2008. Global transcription in pluripotent embryonic stem cells. Cell Stem Cell 2:437–447.

Esteban, M.A., T. Wang, B. Qin, J. Yang, D. Qin, J. Cai, W. Li, Z. Weng, J. Chen, S. Ni, et al, 2010. Vitamin C enhances the generation of mouse and human induced pluripotent stem cells. Cell Stem Cell 6:71–79.

Evans, M. J., & Kaufman, M. H., 1981. Establishment in culture of pluripotential cells from mouse embryos. Nature 292:154-156.

Fazzio, T.G., Huff, J.T., and Panning, B., 2008. An RNAi screen of chromatin proteins identifies Tip60-p400 as a regulator of embryonic stem cell identity. Cell 134:162–174.

Feng, B., J. Jiang, P. Kraus, J.-H. Ng, Heng J.-C.D., Y.-S. Chan, L.-P. Yaw, W. Zhang, Y.-H. Loh, J. Han, et al, 2009. Reprogramming of fibroblasts into induced pluripotent stem cells with orphan nuclear receptor Esrrb. Nat Cell Biology 11:197–203.

Fierz, B., Chatterjee, C., McGinty, R.K., Bar-Dagan, M., Raleigh, D.P., and Muir, T.W., 2011. Histone H2B ubiquitylation disrupts local and higher-order chromatin compaction. Nat. Chem. Biol. 7:113–119

Jan, S. Z., Hamer, G., Repping, S., de Rooij, D. G., van Pelt, A. M., & Vormer, T. L., 2012. Molecular control of rodent spermatogenesis. Biochimica et Biophysica Acta (BBA)-Molecular Basis of Disease, 1822:1838-1850.

Jang, C. W., Shibata, Y., Starmer, J., Yee, D., and Magnuson, T., 2015. Histone H3. 3 maintains genome integrity during mammalian development. Genes & development, 29(13), 1377-1392.

Jauch, R., I. Aksoy, A.P. Hutchins, C.K.L. Ng, X.F. Tian, J. Chen, P. Palasingam, P. Robson, L.W. Stanton, P.R. Kolatkar, 2011. Conversion of Sox17 into a pluripotency reprogramming factor by reengineering its association with Oct4 on DNA. Stem Cells 29:940–951.

Gafni, O., Weinberger, L., Mansour, A.A., Manor, Y.S., Chomsky, E., Ben-Yosef, D., Kalma, Y., Viukov, S., Maza, I., Zviran, A., Rais, Y., Shipony, Z., Mukamel, Z., Krupalnik, V., Zerbib, M., Geula, S., Caspi, I., Schneir, D., Shwartz, T., Gilad, S., Amann-Zalcenstein, D., Benjamin, S., Amit, I., Tanay, A., Massarwa, R., Novershtern, N.,

Hanna, J.H., 2013. Derivation of novel human ground state naive pluripotent stem cells. Nature 504:282–286.

Gaucher, J., Reynoird, N., Montellier, E., Boussouar, F., Rousseaux, S., & Khochbin, S., 2010. From meiosis to postmeiotic events: the secrets of histone disappearance. FEBS journal 277: 599-604.

Gardner, R. L., & Beddington, R. S. P., 1988. Multi-lineage ‘stem’cells in the mammalian embryo. Journal of Cell Science 1988(Supplement 10) :11-27.

Gaspar-Maia, A., Alajem, A., Polesso, F., Sridharan, R., Mason, M.J., Heidersbach, A., Ramalho-Santos, J., McManus, M.T., Plath, K., Meshorer, E., and Ramalho-Santos, M., 2009. Chd1 regulates open chromatin and pluripotency of embryonic stem cells. Nature 460:863–868.

Gaspar-Maia, A., Alajem, A., Meshorer, E., and Ramalho-Santos, M., 2011. Open chromatin in pluripotency and reprogramming. Nature reviews Molecular cell biology 12: 36-47.

Golipour, O., L. David, Y. Liu, G. Jayakumaran, C.L. Hirsch, D. Trcka, J.L. Wrana, 2012. A late transition in somatic cell reprogramming requires regulators distinct from the pluripotency network. Cell Stem Cell 11:769–782.

Govin, J., Escoffier, E., Rousseaux, S., Kuhn, L., Ferro, M., Thévenon, J.,et al., 2007. Pericentric heterochromatin reprogramming by new histone variants during mouse spermiogenesis. The Journal of cell biology 176: 283-294.

Gropp, M., Shilo, V., Vainer, G., Gov, M., Gil, Y., Khaner, H., Matzrafi, L., Idelson, M., Kopolovic, J., Zak, N.B., Reubinoff, B.E., 2012. Standardization of the teratoma assay for analysis of pluripotency of human ES cells and biosafety of their differentiated progeny. PLOS ONE 7: e45532.

Gurdon, J.B., Elsdale, T.R., Fischberg, M., 1958. Sexually mature individuals of Xenopus laevis from the transplantation of single somatic nuclei. Nature 182:64–65.

Gurard-Levin, Z. A., Quivy, J. P., & Almouzni, G., 2014. Histone chaperones: assisting histone traffic and nucleosome dynamics. Annual review of biochemistry 83:487-517.

Hess, R. A. and Renato de Franca, L., 2008. Spermatogenesis and cycle of the seminiferous epithelium. Adv. Exp. Med. Biol. 636:1–15.

Heng J-C.D, B. Feng, J. Han, J. Jiang, P. Kraus, J.-H. Ng, Y.L. Orlov, M. Huss, L. Yang, T. Lufkin, et al., 2010. The nuclear receptor Nr5a2 can replace Oct4 in the reprogramming of murine somatic cells to pluripotent cells. Cell Stem Cell 6:167–174.

Hou, P., Y. Li, X. Zhang, C. Liu, J. Guan, H. Li, T. Zhao, J. Ye, W. Yang, K. Liu, et al., 2013. Pluripotent stem cells induced from mouse somatic cells by small-molecule compounds. Science 341:651–654.

Huang, H.D., Lee, T.Y., Tzeng, S.W., Horng, J.T., 2005. KinasePhos: a web tool for identifying protein kinase-specific phosphorylation sites. Nucleic Acds Res. 33:W226–W229.

Huangfu, D., Maehr, R., Guo, W., Eijkelenboom, A., Snitow, M., Chen, A. E., and Melton, D. A., 2008. Induction of pluripotent stem cells by defined factors is greatly improved by small-molecule compounds. Nature biotechnology 26 : 795-797.

Iwasaki, W., Miya, Y., Horikoshi, N., Osakabe, A., Taguchi, H., Tachiwana, H., and Kurumizaka, H.., 2013. Contribution of histone N-terminal tails to the structure and stability of nucleosomes. FEBS open bio, 3, 363-369.

K. Inoue, T. Kohda, M. Sugimoto, T. Sado, N. Ogonuki, S. Matoba, H. Shiura, R. Ikeda, K. Mochida, T. Fujii, et al., 2010. Impeding Xist expression from the active X chromosome improves mouse somatic cell nuclear transfer. Science 330 :496–499

Kaufman, M. H., & Kaufman, M. H., 1992. The atlas of mouse development (Vol. 428). San Diego:: Academic press.

Kawamura, T., Suzuki, J., Wang, Y. V., Menendez, S., Morera, L. B., Raya, A. et al., 2009. Linking the p53 tumour suppressor pathway to somatic cell reprogramming. Nature 460:1140-1144.

Koyanagi-Aoi, M., Ohnuki, M., Takahashi, K., Okita, K., Noma, H., Sawamura, Y., Teramoto, I., Narita, M., Sato, Y., Ichisaka, T., Amano, N., Watanabe, A., Morizane, A., Yamada, Y., Sato, T., Takahashi, J., Yamanaka, S., 2013. Differentiation-defective phenotypes revealed by large-scale analyses of human pluripotent stem cells. Proc. Natl. Acad. Sc. USA 110:20569–20574.

Lapasset, L., Milhavet, O., Prieur, A., Besnard, E., Babled, A., Aït-Hamou, N., et al., 2011. Rejuvenating senescent and centenarian human cells by reprogramming through the pluripotent state. Genes & development 25: 2248-2253.

Laskey, R. A., Honda, B. M., Mills, A. D., & Finch, J. T., 1978. Nucleosomes are assembled by an acidic protein which binds histones and transfers them to DNA. Nature 275:416-420.

Li, A., Maffey, A.H., Abbott, W.D., Conde E Silva, N., Prunell, A., Siino, J., Churikov, D., Zalensky, A.O., Ausió, J., 2005. Characterization of nucleosomes consisting of the human testis/sperm-specific histone H2B variant (hTSH2B). Biochemistry 44:2529–2535.

Lister, R., Pelizzola, M., Kida, Y. S., Hawkins, R. D., Nery, J. R., Hon, G., et al., 2011. Hotspots of aberrant epigenomic reprogramming in human induced pluripotent stem cells. Nature, 471: 68-73.

Lu, L.Y., J. Wu, L. Ye, G.B. Gavrilina, T.L. Saunders, X. Yu, 2010. RNF8-dependent histone modifications regulate nucleosome removal during spermatogenesis. Dev Cell 18:371–384.

Luo, M., T. Ling, W. Xie, H. Sun, Y. Zhou, Q. Zhu, M. Shen, L. Zong, G. Lyu, Y. Zhao, et al., 2013. NuRD blocks reprogaramming of mouse somatic cells into pluripotent stem cells. Stem Cells 31:1278–1286

Mali, P., B.K. Chou, J. Yen, Z. Ye, J. Zou, S. Dowey, R.A. Brodsky, J.E. Ohm, W. Yu, S.B. Baylin, et al., 2010. Butyrate greatly enhances derivation of human induced pluripotent stem cells by promoting epigenetic remodeling and the expression of pluripotency-associated genes. Stem Cells 28:713-20.

Ma, H., Morey, R., O'Neil, R.C., He, Y., Daughtry, B., Schultz, M.D., Hariharan, M., Nery, J.R., Castanon, R., Sabatini, K., Thiagarajan, R.D., Tachibana, M., Kang, E., Tippner-Hedges, R., Ahmed, R., Gutierrez, N.M., Van Dyken, C., Polat, A., Sugawara, A., Sparman, M., Gokhale, S., Amato, P., Wolf, D.P., Ecker, J.R., Laurent, L.C., Mitalipov, S., 2014. Abnormalities in human pluripotent cells due to reprogramming mechanisms. Nature 511:177–183.

Maekawa M., K. Yamaguchi, T. Nakamura, R. Shibukawa, I. Kodanaka, T. Ichisaka, Y. Kawamura, H. Mochizuki, N. Goshima, S. Yamanaka, 2011. Direct reprogramming of somatic cells is promoted by maternal transcription factor Glis1. Nature 474:225–229.

Mansour, A.A., O. Gafni, L. Weinberger, A. Zviran, M. Ayyash, Y. Rais, V. Krupalnik, M. Zerbib, D. Amann-Zalcenstein, I. Maza, et al., 2012. The H3K27 demethylase Utx regulates somatic and germ cell epigenetic reprogramming. Nature, 488:409–413.

Martin, G. R., 1981. Isolation of a pluripotent cell line from early mouse embryos cultured in medium conditioned by teratocarcinoma stem cells. Proceedings of the National Academy of Sciences 78: 7634-7638.

Meistrich, M.L., P.K. Trostle-Weige, R. Lin, Y.M. Bhatnagar, C.D., 1992. Allis Highly acetylated H4 is associated with histone displacement in rat spermatids. Mol. Reprod. Dev., 31:170–181.

Meistrich, M.L., B. Mohapatra, C.R. Shirley, M. Zhao, 2003. Roles of transition nuclear proteins in spermiogenesis. Chromosoma, 111:483–488.

Mikkelsen, T. S., Hanna, J., Zhang, X., Ku, M., Wernig, M., Schorderet, P., et al., 2008. Dissecting direct reprogramming through integrative genomic analysis. Nature, 454:49-55.

Mills, A. D., Laskey, R. A., Black, P., and De Robertis, E. M., 1980. An acidic protein which assembles nucleosomes in vitro is the most abundant protein in Xenopus oocyte nuclei. Journal of molecular biology 139: 561-568.

Montellier, E., Boussouar, F., Rousseaux, S., Zhang, K., Buchou, T., Fenaille, F., Shiota, H., Debernardi, A., Héry, P., Curtet, S., Jamshidikia, M., Barral, S., Holota, H., Bergon, A., Lopez, F., Guardiola, P., Pernet, K., Imbert, J., Petosa, C., Tan, M., Zhao, Y., Gérard, M., and Khochbin, S., 2013. Chromatin-to-nucleoprotamine transition is controlled by the histone H2B variant TH2B. Genes Dev. 27:1680–1692.

Moussaieff, A., Rouleau, M., Kitsberg, D., Cohen, M., Levy, G., Barasch, D., and Nahmias, Y., 2015. Glycolysis-mediated changes in acetyl-coA and histone acetylation control the early differentiation of embryonic stem cells. Cell metabolism 21: 392-402.

Montserrat N., E. Nivet, I. Sancho-Martinez, T. Hishida, S. Kumar, L. Miquel, C. Cortina, Y. Hishida, Y. Xia, C.R. Esteban, et al., 2013. Reprogramming of human fibroblasts to pluripotency with lineage specifiers. Cell Stem Cell 13:341–350.

Morris S.A., Cahan P., Li H., Zhao A.M., San Roman A.K., Shivdasani R.A., Collins J.J., Daley G.Q., 2014. Dissecting engineered cell types and enhancing cell fate conversion via Cell Net. Cell 158: 889–902.

Nakagawa M., M. Koyanagi, K. Tanabe, K. Takahashi, T. Ichisaka, T. Aoi, K. Okita, Y. Mochiduki, N. Takizawa, S. Yamanaka, et al., 2008. Generation of induced pluripotent stem cells without Myc from mouse and human fibroblasts. Nat Biotech 26:101–106.

Nashun, B., Hill, P. W., and Hajkova, P., 2015. Reprogramming of cell fate: epigenetic memory and the erasure of memories past. The EMBO journal, e201490649.

Nichols, J., Smith. A., 2009. Naive and primed pluripotent states. Cell Stem Cell 4:487–492.

Ohi, Y., Qin, H., Hong, C., Blouin, L., Polo, J.M., Guo, T., Qi, Z., Downey, S.L., Manos, P.D., Rossi, D.J., Yu, J., Hebrok, M., Hochedlinger, K., Costello, J.F., Song, J.S., Ramalho-Santos, M., 2011. Incomplete DNA methylation underlies a transcriptional memory of somatic cells in human iPS cells. Nat. Cell Biol. 13:541–549.

Ohtsuka, S., Nakai-Futatsugi, Y., and Niwa, H., 2015. LIF signal in mouse embryonic stem cells. JAK-STAT, 4(2), 1-19.

Okita, K., Ichisaka, T., & Yamanaka, S., 2007. Generation of germline-competent induced pluripotent stem cells. Nature 448: 313-317.

Oliva, R., Bazett-Jones, D., Mezquita, C., & Dixon, G. H., 1987. Factors affecting nucleosome disassembly by protamines in vitro. Histone hyperacetylation and chromatin structure, time dependence, and the size of the sperm nuclear proteins. Journal of Biological Chemistry 262: 17016-17025.

Onder, T.T, N. Kara, A. Cherry, A.U. Sinha, N. Zhu, K.M. Bernt, P. Cahan, O.B. Mancarci, J. Unternaehrer, P.B. Gupta, et al., 2012. Chromatin-modifying enzymes as modulators of reprogramming. Nature 483:598–602.

Panopoulos, A. D., Ruiz, S., Yi, F., Herrerías, A., Batchelder, E. M., & Izpisua Belmonte, J. C., 2011. Rapid and highly efficient generation of induced pluripotent stem cells from human umbilical vein endothelial cells. PloS one 6: e19743.

Panopoulos, A. D., Yanes, O., Ruiz, S., Kida, Y. S., Diep, D., Tautenhahn, R.et al., 2012. The metabolome of induced pluripotent stem cells reveals metabolic changes occurring in somatic cell reprogramming. Cell research, 22:168-177.

Pasque, V., Radzisheuskaya, A., Gillich, A., Halley-Stott, R. P., Panamarova, M., Zernicka-Goetz, M., and Silva, J. C., 2012. Histone variant macroH2A marks embryonic differentiation in vivo and acts as an epigenetic barrier to induced pluripotency. Journal of cell science, 125(24), 6094-6104.

Parra, M. A., Kerr, D., Fahy, D., Pouchnik, D. J., and Wyrick, J. J., 2006. Deciphering the roles of the histone H2B N-terminal domain in genome-wide transcription. Molecular and cellular biology, 26(10), 3842-3852.

Philpott, A., Leno, G. H., and Laskey, R. A., 1991. Sperm decondensation in Xenopus egg cytoplasm is mediated by nucleoplasmin. Cell 65: 569-578.

Pijnappel, W.W.M.P., D. Esch, M.P.A. Baltissen, G. Wu, N. Mischerikow, A.J. Bergsma, E. van der Wal, D.W. Han, H. vom Bruch, S. Moritz, et al., 2013. A central role for TFIID in the pluripotent transcription circuitry. Nature 495:516–519.

Rais, Y., A. Zviran, S. Geula, O. Gafni, E. Chomsky, S. Viukov, A.A. Mansour, I. Caspi, V. Krupalnik, M. Zerbib, et al., 2013. Deterministic direct reprogramming of somatic cells to pluripotency. Nature 502:65–70.

Rao, B.J., Brahmachari, S.K., and Rao, M.R.S., 1983. Structural organization of the meiotic prophase chromatin in the rat testis. J. Biol. Chem. 258:13478–13485.

Rossant, J., 2008. Stem cells and early lineage development. Cell 132: 527-531.

Romrell, L. J., Bellvé, A. R., & Fawcett, D. W., 1976. Separation of mouse spermatogenic cells by sedimentation velocity: a morphological characterization. Developmental biology 49:119-131.

Santoro, S. W., & Dulac, C., 2015. Histone variants and cellular plasticity. Trends in Genetics 31:31516–527

Shirley, C.R., S. Hayashi, S. Mounsey, R. Yanagimachi, M.L. Meistrich, 2004. Abnormalities and reduced reproductive potential of sperm from Tnp1- and Tnp2-null double mutant mice. Biol. Reprod. 71:1220–1229.

Shinagawa, T., Huynh, L.M., Takagi, T., Tsukamoto, D., Tomaru, C., Kwak, H.G., Dohmae, N., Noguchi, J., Ishii, S., 2015. Disruption of Th2a and Th2b genes causes defects in spermatogenesis. Development 142:1287–1292.

Shinagawa, T., Takagi, T., Tsukamoto, D., Tomaru, C., Huynh, L.M., Sivaraman, P., Kumarevel, T., Inoue, K., Nakato, R., Katou, Y., Sado, T., Takahashi, S., Ogura, A.,

Shirahige, K., Ishii, S., 2014. Histone variants enriched in oocytes enhance reprogramming to induced pluripotent stem cells. Cell Stem Cell 14:217–227.

Shires, A., Carpenter, M. P., & Chalkley, R., 1976. A cysteine-containing H2B-like histone found in mature mammalian testis. Journal of Biological Chemistry 251: 4155-4158.

Shu J., C. Wu, Y. Wu, Z. Li, S. Shao, W. Zhao, X. Tang, H. Yang, L. Shen, X. Zuo, et al., 2013. Induction of pluripotency in mouse somatic cells with lineage specifiers. Cell 153:963–975

Singhal, N., Graumann, J., Wu, G., Araúzo-Bravo, M. J., Han, D. W., Greber, B., et al., 2010. Chromatin-remodeling components of the BAF complex facilitate reprogramming. Cell 141:943-955.

Soufi. A., G. Donahue, K.S. Zaret, 2012. Facilitators and impediments of the pluripotency reprogramming factors' initial engagement with the genome. Cell 151:994–1004.

Soufi, A., 2014. Mechanisms for enhancing cellular reprogramming. Current opinion in genetics & development 25:101-109.

Spiridonov, N.A, L. Wong, P.M. Zerfas, M.F. Starost, S.D. Pack, C.P. Paweletz, G.R. Johnson, 2005. Identification and characterization of SSTK, a serine/threonine protein kinase essential for male fertility. Mol. Cell. Biol. 25:4250–4261.

Subramanian, A., Tamayo, P., Mootha, V.K., Mukherjee, S., Ebert, B.L., Gillette, M.A., Paulovich, A., Pomeroy, S.L., Golub, T.R., Lander, E.S., Mesirov, J.P., 2005. Gene set enrichment analysis: A knowledge-based approach for interpreting genome-wide expression profiles. Proc. Natl. Acad. Sci. USA 102:15545–15550.

Sridharan, R., M. Gonzales-Cope, C. Chronis, G. Bonora, R. McKee, C. Huang, S. Patel, D. Lopez, N. Mishra, M. Pellegrini, et al., 2013. Proteomic and genomic approaches reveal critical functions of H3K9 methylation and heterochromatin protein-1γ in reprogramming to pluripotency. Nat Cell Biol, 7:872–882.

Stadtfeld, M., E. Apostolou, F. Ferrari, J. Choi, R.M. Walsh, T. Chen, S.S.K. Ooi, S.Y. Kim, T.H. Bestor, T. Shioda, et al., 2012. Ascorbic acid prevents loss of Dlk1-Dio3 imprinting and facilitates generation of all-iPS cell mice from terminally differentiated B cells. Nat Genet 44:S1–S2.

Tachiwana, H., Kagawa, W., Osakabe, A., Kawaguchi, K., Shiga, T., Hayashi-Takanaka, Y., Kimura, H., and Kurumizaka, H., 2010. Structural basis of instability of the nucleosome containing a testis-specific histone variant, human H3T. Proc. Natl. Acad. Sci. USA 107:10454–10459.

Takahashi, K., Tanabe, K., Ohnuki, M., Narita, M., Ichisaka, T., Tomoda, K., Yamanaka, S., 2007. Induction of pluripotent stem cells from adult human fibroblasts by defined factors. Cell 131:861–872

Takahashi, K., Yamanaka, S., 2006. Induction of pluripotent stem cells from mouse embryonic and adult fibroblast cultures by defined factors. Cell 126:663–676.

Takashima, Y., Guo, G., Loos, R., Nichols, J., Ficz, G., Krueger, F., Oxley, D., Santos, F., Clarke, J., Mansfield, W., Reik, W., Bertone, P., Smith, A., 2014. Resetting transcription factor control circuitry toward ground-state pluripotency in human. Cell 158:1254–1269.

Tesar, P.J., Chenoweth, J.G., Brook, F.A., Davies, T.J., Evans, E.P., Mack, D.L., Gardner, R.L., McKay, R.D., 2007. New cell lines from mouse epiblast share defining features with human embryonic stem cells. Nature 448:196–199.

Theunissen, T.W., Powell, B.E., Wang, H., Mitalipova, M., Faddah, D.A., Reddy, J., Fan, Z.P., Maetzel, D., Ganz, K., Shi, L., Lungjangwa, T., Imsoonthornruksa, S., Stelzer, Y., Rangarajan, S., D'Alessio, A., Zhang, J., Gao, Q., Dawlaty, M.M., Young, R.A., Gray, N.S., Jaenisch, R., 2014. Systematic identification of culture conditions for induction and maintenance of naive human pluripotency. Cell Stem Cell 15:471–487.

Thomson, J. A., Itskovitz-Eldor, J., Shapiro, S. S., Waknitz, M. A., Swiergiel, J. J., Marshall, V. S., & Jones, J. M., 1998. Embryonic stem cell lines derived from human blastocysts. Science 282:1145-1147.

Trostle-Weige, P. K., Meistrich, M. L., Brock, W. A., Nishioka, K., & Bremer, J. W., 1982. Isolation and characterization of TH2A, a germ cell-specific variant of histone 2A in rat testis. Journal of Biological Chemistry 257:5560-5567.

Tsubouchi, T., Soza-Ried, J., Brown, K., Piccolo, F. M., Cantone, I., Landeira, D., ... and Fisher, A. G., 2013. DNA synthesis is required for reprogramming mediated by stem cell fusion. Cell, 152(4), 873-883.

Wakayama, T., Perry, A.C., Zuccotti, M., Johnson, K.R., Yanagimachi, R., 1998. Full-term development of mice from enucleated oocytes injected with cumulus cell nuclei. Nature 394:369–374.

Ware, C.B., Nelson, A.M., Mecham, B., et al. 2014. Derivation of naive human embryonic stem cells. Proc. Natl. Acad. Sci. USA 111:4484–4489.

Wernig, M., Meissner, A., Foreman, R., Brambrink, T., Ku, M., Hochedlinger, K.,et al., 2007. In vitro reprogramming of fibroblasts into a pluripotent ES-cell-like state. Nature 448:318-324.

Wernig M., A. Meissner, J.P. Cassady, R. Jaenisch, 2008. c-Myc is dispensable for direct reprogramming of mouse fibroblasts. Cell Stem Cell 2:10–12.

Vogler, C., Huber, C., Waldmann, T., Ettig, R., Braun, L., Izzo, A., ... and Dundr, M., 2010. Histone H2A C-terminus regulates chromatin dynamics, remodeling, and histone H1 binding. Plos One: e1001234.

Xia, X., Zhang, Y., Zieth, C.R., Zhang, S.C., 2007. Transgenes delivered by lentiviral vector are suppressed in human embryonic stem cells in a promoter-dependent manner. Stem Cell Dev. 16:167–176.

Yan, L., Yang, M., Guo, H., Yang, L., Wu, J., Li, R., Liu, P., Lian, Y., Zheng, X., Yan, J., Huang, J., Li, M., Wu, X., Wen, L., Lao, K., Li, R., Qiao, J., Tang, F., 2013. Single-cell RNA-Seq profiling of human preimplantation embryos and embryonic stem cells. Nat. Struct. Mol. Biol. 20:1131–1139.

Yu, Y.E., Y. Zhang, E. Unni, C.R. Shirley, J.M. Deng, L.D. Russell, M.M. Weil, R.R. Behringer, M.L. Meistrich, 2000. Abnormal spermatogenesis and reduced fertility in transition nuclear protein 1-deficient mice. Proc. Natl. Acad. Sci. U. S. A. 97:4683–4688.

Yu, J., Hu, K., Smuga-Otto, K., Tian, S., Stewart, R., Slukvin, I.I., Thomson, J.A., 2009. Human induced pluripotent stem cells free of vector and transgene sequences. Science 324:797–801.

Zalensky, A.O., Siino, J.S., Gineitis, A.A., Zalenskaya, I.A., Tomilin, N.V., Yau, P., Bradbury, E.M., 2002. Human testis/sperm-specific histone H2B (hTSH2B). Molecular cloning and characterization. J. Biol. Chem. 277:43474–43480.

REFERENCE MATERIALS

1. Shinagawa, T., Takagi, T., Tsukamoto, D., Tomaru, C., Huynh, L.M., Sivaraman, P., Kumarevel, T., Inoue, K., Nakato, R., Katou, Y., Sado, T., Takahashi, S., Ogura, A., Shirahige, K., Ishii, S., 2014. Histone variants enriched in oocytes enhance reprogramming to induced pluripotent stem cells. Cell Stem Cell 14:217–227.

2. Shinagawa, T., Huynh, L.M., Takagi, T., Tsukamoto, D., Tomaru, C., Kwak, H.G., Dohmae, N., Noguchi, J., Ishii, S., 2015. Disruption of Th2a and Th2b genes causes defects in spermatogenesis. Development 142:1287–1292.

3. Huynh L.M, Shinagawa, T. and Ishii S., 2016. Stem Cells and Development, ahead of print. doi:10.1089/scd.2015.0264.

Figure legends

Figure 1.1 Developmental process and cellular potency. As the development progresses, cellular potency reduces. Mouse ESCs and human naïve ESCs are closely related to ICM, while epiblast stem cells and human primed ESCs are closed to the post-implantation epiblast stage.

Figure 1.2 Developmental Expression of Histone TH2A and TH2B (Shinagawa et al., 2014) (A) The average levels of *Th2a* and *Th2b* mRNA in various tissues and cells relative to the levels in MEFs are shown ±SD (n = 3). (B) Immunofluorescence images of TH2A/TH2B (red) or Oct3/4 (green) stained oocytes and early embryos. DNA was visualized with DAPI (blue). Regions marked by white squares are shown at a higher magnification. m, male pronucleus; f, female pronucleus; PB, polar body. Scale bars, 50 μm.

Figure 1.3 The efficiency of reprogramming by TH2A, TH2B and P-NPM2. **(Shinagawa et al., 2014)** *Nanog*-GFP MEFs (male) were infected with retroviruses to express the indicated factors, and the percentage of GFP^+ cells was analyzed using FACS on day 10 postinfection The mean is indicated by a green bar. Exp., experiment.

Figure 1.4 Summary of TH2A/TH2B enhancing iPSC generation in mouse MEFs (Shingawa et al., 2014).

Figure 2.1 Expression and deposition of TH2A/TH2B into chromatin. Using NIH3T3 cells expressing TH2A/TH2B and P-Npm or H2A/H2B and P-Npm, or containing control empty vector, the expression levels (a) and deposition into chromatin (b) of the indicated histones were examined.

Figure 2.2 Increase in DNase I sensitivity induced by TH2A/TH2B. Nuclei prepared from NIH3T3 cells expressing the indicated proteins were incubated with DNase I for the indicated time, and the average amount of digested DNA is shown ± SD (n = 3).

Figure 2.3 MNase sensitivity was not affected by TH2A/TH2B. Nuclei were prepared from two types of NIH3T3 cells expressing the empty vectors, TH2A/TH2B and P-Npm, or H2A/H2B and P-Npm. Nuclei were treated with various amounts of MNase, and the digested DNA was analyzed by agarose gel electrophoresis.

Figure 2.4 The total amount of histone H3K9me3 was not affected by TH2A/TH2B. (Left panel) Using ELISA, the amount of histone H3K9me3 was measured using various amounts of the histone fraction (R-squared = 0.96). (Right panel) The amount of histone H3K9me3 was measured using a chromatin fraction prepared from NIH3T3 cells expressing TH2A/TH2B/P-Npm or H2A/H2B/P-Npm, or one prepared from cells infected with empty vector. For the positive and negative controls, chromatin fractions enriched in tight heterochromatin (inactive chromatin) or enriched in euchromatin (active chromatin) were used. The relative average level of H3K9me3 compared with that of control NIH3T3 cells is shown ± SD (n = 3). N.S., no significant difference.

Figure 2.5 Histone H3K9me3 signals were not affected by TH2A/TH2B. NIH3T3 cells expressing TH2A/TH2B/P-Npm or H2A/H2B/P-Npm were immunostained with anti-H3K9me3 (red) or anti-TH2B (green). DNA was stained with TO-PRO-3. The image surrounded by a white box is shown at a higher magnification. The merged images are shown in the panels at the right.

Figure 2.6 Defects in histone replacement during spermiogenesis in *Th2a-/-Th2b-/-* mice. (A) Testis sections were immunostained with anti-TNP2 (green) and anti-γH2AX (red) antibodies. The stage of the seminiferous epithelial cycle was judged by the morphology of spermatids and the staining pattern of γH2AX. (B) Representative immunostaining images of spermatids are shown. The abnormal nuclear morphology is marked by blue triangles. (C) Spermatid lysates were separated by centrifugation into supernatant (non-chromatin) and pellet (chromatin) fractions, and were used for western blotting.

Figure 2.7 Comparison of mRNA levels of genes that are typically transcribed in spermatids in wild-type (+/+) and mutant (-/-) testes. The mRNA levels are shown as an average of three measurements (± SD (n = 3)). N.S., not significant.

Figure 2.8 Levels of canonical and variant histones of H2A and H2B in spermatids. Round and elongating spermatids were isolated from wild-type and mutant testes, and whole cell lysates were used for western blotting. A three-fold serial dilution of proteins was used for H2A, while a two-fold serial dilution of proteins was used for the others.

Figure 3.1 Gene structure and amino acid sequences of human histone variants TH2A and TH2B. (Upper) Structure of human *TH2A* and *TH2B* genes. The direction of

transcription is shown by arrow, and the putative binding sites for transcription factors are indicated. (Lower) Amino acid sequences of canonical histone H2A (NP_066390.1), H2B (NP_003509.1) and histone variants TH2A (NP_734466.1), TH2B (NP_733759.1) were aligned. Different amino acids are shown in red color.

Figure 3.2 TH2A and TH2B and histone chaperone P-NPM2 enhanced human iPSC generation from human umbilical vein endothelial cells. (A)The number of TRA-1-60-positivecolonies induced by OSKM or OSKM plus TH2A/TH2B/P-NPM2 (OSKMBAN). Human umbilical vein endothelial cells (HUVECs) were infected with lentiviruses to express indicated proteins, and stained with anti-TRA-1-60 antibody at day 11 post infection (n=3, mean ± SD). Immunostaining of a colony induced by OSKMBAN were shown in the right panel. (B)Representative alkaline phosphatase staining of colonies at day 16 post infection. (C)The number of SSEA4-positive colony from HUVECs induced by OSKM or OSKMBAN at day 11post infection (n=4, mean ± SD).

Figure 3.3 TH2A and TH2B and histone chaperone P-NPM2 enhanced human iPSC generation from human fibroblasts. (A) The number of SSEA4-positive colony from adult human dermal fibroblasts (HDFs) induced by OSKM or OSKMBAN at day 16 post infection (n=4, mean ± SD).

(B) The number of SSEA4-positive colony from neonatal human dermal fibroblasts (nHDFs) induced by OSKM or OSKMBAN at day 16 post infection (n=3, mean ± SD).

Figure 3.4 Prolong expression of BAN further enhance reprogramming Adult HDFs were infected with virus to express BAN or empty vector 5 days before infection with OSKM viruses. The number of SSEA4-positive colony at day 16 post OSKM virus infection is shown (n = 3, mean ± SD).

Figure 3.5 Immunofluorescence staining of pluripotency markers in iPSCs from HDFs generated by OSKMBAN. iPSCs are stained with anti-NANOG (red) and anti-OCT4 (green) antibodies, and DAPI (blue).

Figure 3.6 Cell proliferation rate of OSKM, OSKMBAN, BAN and empty vector overexpressing human fibroblasts was monitored at indicated days.* indicates p-value ≤ 0.05, ** indicates p-value ≤ 0.001.

Figure 3.7 *In vitro* differentiation of iPSCs. OSKMBAN-induced iPSCs were cultured in differentiation medium. Immunostaining of beta-III tubulin (TUJ1) for ectoderm, smooth muscle actin (SMA) for mesoderm, and alpha-fetoprotein (AFP) for endoderm are shown.Scale bar: 100μm.

Figure 3.8 Timing and size of teratoma generated from individual iPSC clones. Grade 0: no teratoma, Grade 1: <0.5 cm^3, Grade 2: >0.5 cm^3.

Figure 3.9 *In vivo* differentiation of iPSCs. (Upper) Hematoxylin and eosin staining of teratoma sections. OSKMBAN-induced iPSCs generated well-differentiated teratomas containing all three germ layers. Typical morphologies of chondrocyte (mesoderm), neural rosette (ectoderm), and epithelial-like structure (endoderm) are shown. Scale bar: 100μm. (Lower) Teratomas were positive for differentiation markers for three germ layers: SMA, TUJ1, and AFP. Scale bar: 100μm.

Figure 3.10 OSKMBAN-induced iPSCs showed higher differentiation capacity than OSKM-induced iPSCs The size of area of epithelial-like structure in each three OSKM- and OSKMBAN-teratomas was measured as in (A), and shown in the boxplot (B and C). Total number of the area of epithelial-like structures analyzed in OSKM- and OSKMBAN-teratomas are 320 and 318, respectively. Middle lines in the box indicates medians; top and bottom edges, the lower and upper quartiles (25% and 75%); and whiskers, minimum and maximum values; circles are outline values. ** indicates p-value < 0.001.

Figure 3.11 Global gene expression profile of OSKMBAN-induced iPSCs are clustered with OSKM-induced iPSCs and human ESCs. Hierarchical cluster analysis of microarray expression data from three ES cell lines, each of three clones of OSKM-induced iPSCs and OSKMBAN-induced iPSCs, and three fibroblasts. Microarray data for human ESCs and human fibroblasts were obtained from Ohi et al. (2011).

Figure 3.12 Scatterplots of global gene expression patterns, comparing the indicated types of cells (average expression of three clones). The expression levels of some pluripotent markers (OCT4, SOX2, NANOG, ZFP42, and GDF3) are shown in red.

Figure 3.13 Expression of endogenous *OCT4*, *NANOG*, and *GDF3* mRNAs in OSKMBAN-induced iPSCs was compared to that in OSKM-induced iPSCs or HDFs. Data shown as mean ± SD (n = 3). NS indicates no significant different.

Figure 3.14 Exogenous expression of cMYC and SOX2 in human iPSC clones. (Upper panel) Exogeneous cMYC expression and (Lower panel) exogenous SOX2 expression were measured by qRT-PCR and normalized to GAPDH, n = 3. Expression at 4 days post infection was used as control.

Figure 3.15 Gene set enrichment analysis of OSKM- and OSKMBAN-induced iPSCs. Up-regulated genes in OSKMBAN-induced iPSCs compared to OSKM-induced iPSCs are shown (q value <0.1).

Figure 3.16 GSEA analysis for OSKMBAN- and OSKM-induced iPSCs probe sets with up- and down-regulated transcripts of naïve pluripotent stem cells compared to primed pluripotent stem cells. Four fold up- or down-regulated transcripts were retrieved from Theunissen et al. (2014).

Figure 1.1

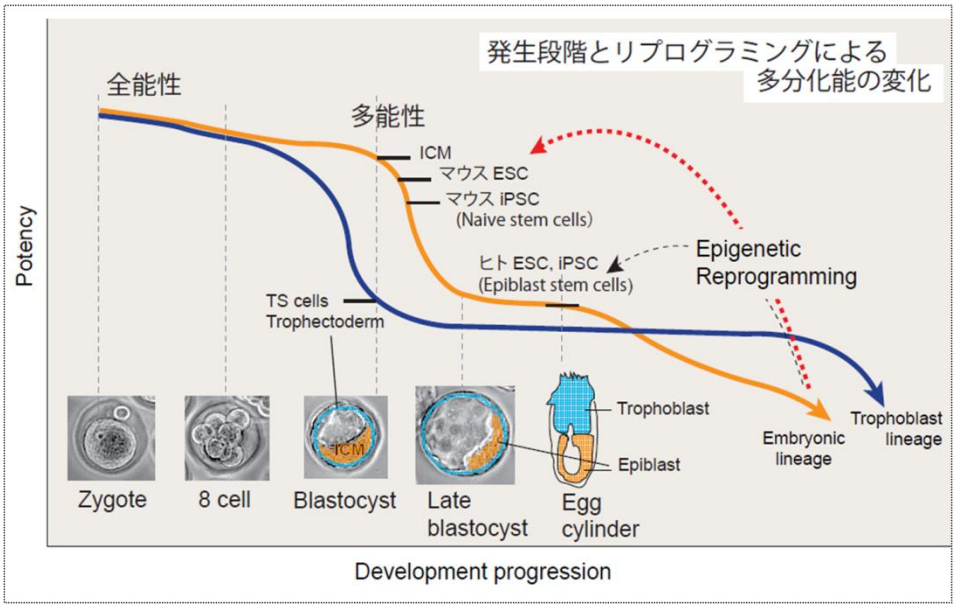
発生段階とリプログラミングによる
多分化能の変化
全能性
多能性
ICM
マウス ESC
マウス iPSC
(Naive stem cells)
ヒト ESC, iPSC
(Epiblast stem cells)
Epigenetic
Reprogramming
TS cells
Trophectoderm
Potency
Trophoblast
Epiblast
Embryonic
lineage
Trophoblast
lineage
ICM
Zygote
8 cell
Blastocyst
Late
blastocyst
Egg
cylinder
Development progression

Figure 1.2

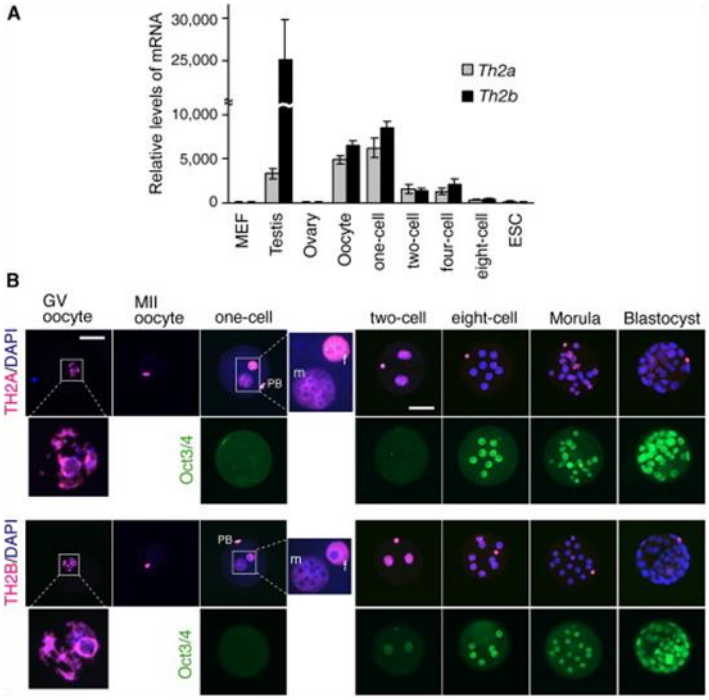
A
Relative levels of mRNA
30,000
25,000
10,000
5,000
0
Th2a
Th2b
MEF
Testis
Ovary
Oocyte
one-cell
two-cell
four-cell
eight-cell
ESC
B
GV oocyte
MII oocyte
one-cell
two-cell
eight-cell
Morula
Blastocyst
TH2A/DAPI
TH2B/DAPI
Oct3/4
PB
m
p

Figure 1.3

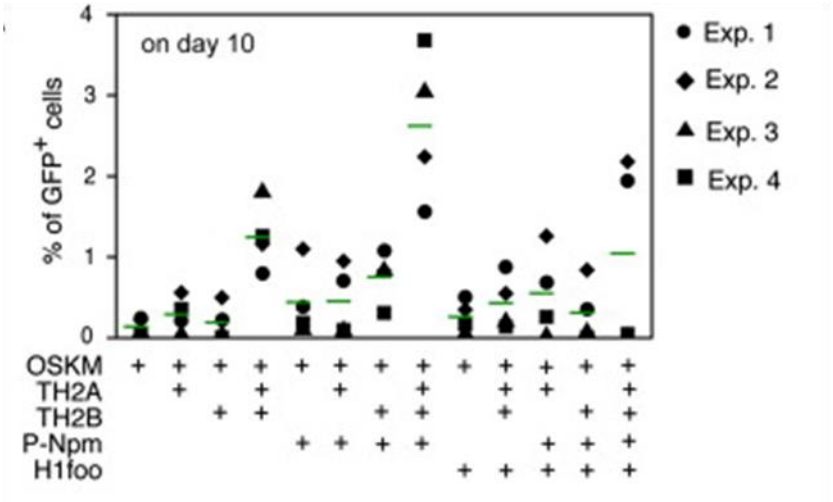
on day 10
% of GFP+ cells
0
1
2
3
4
OSKM
TH2A
TH2B
P-Npm
H1foo
Exp. 1
Exp. 2
Exp. 3
Exp. 4

Figure 1.4

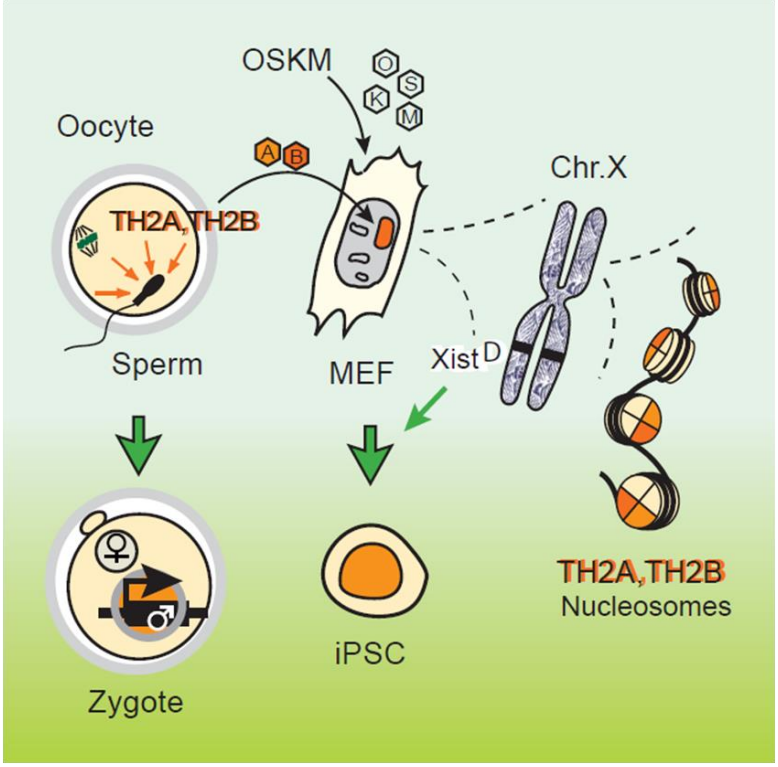
OSKM
O
S
K
M
Oocyte
A
B
Chr.X
TH2A,TH2B
Sperm
MEF
Xist D
TH2A,TH2B
Nucleosomes
iPSC
Zygote

Figure 2.1

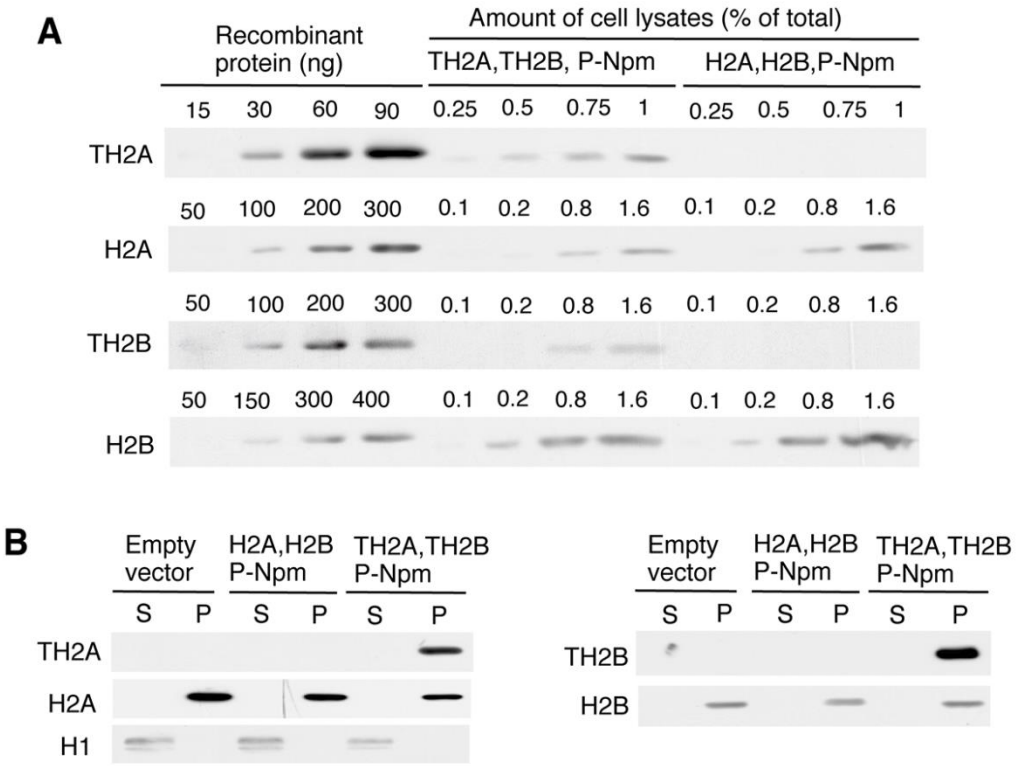
A
Recombinant protein (ng)
Amount of cell lysates (% of total)
TH2A,TH2B, P-Npm
H2A,H2B,P-Npm
15 30 60 90 0.25 0.5 0.75 1 0.25 0.5 0.75 1
TH2A
50 100 200 300 0.1 0.2 0.8 1.6 0.1 0.2 0.8 1.6
H2A
50 100 200 300 0.1 0.2 0.8 1.6 0.1 0.2 0.8 1.6
TH2B
50 150 300 400 0.1 0.2 0.8 1.6 0.1 0.2 0.8 1.6
H2B
B
Empty vector
H2A,H2B P-Npm
TH2A,TH2B P-Npm
S P S P S P
TH2A
H2A
H1
Empty vector
H2A,H2B P-Npm
TH2A,TH2B P-Npm
S P S P S P
TH2B
H2B

Figure 2.2

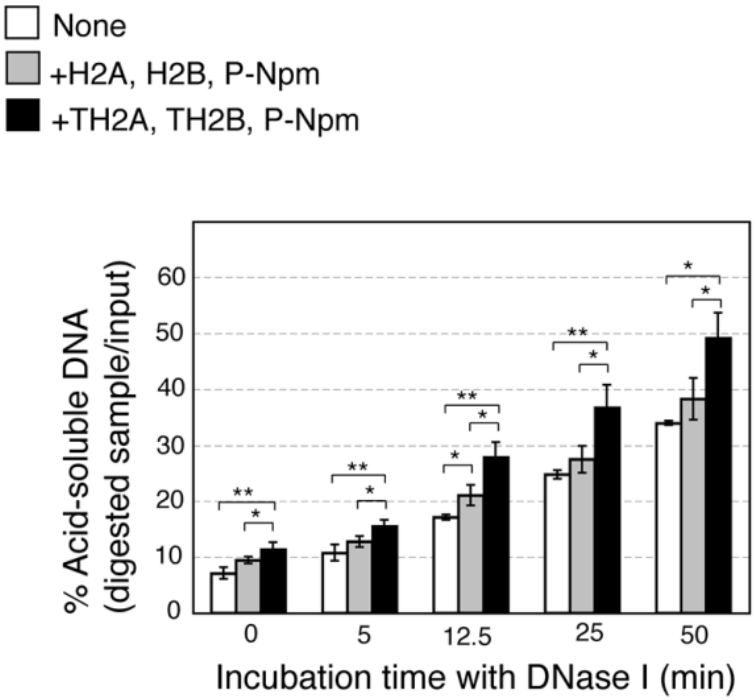
None
+H2A, H2B, P-Npm
+TH2A, TH2B, P-Npm
% Acid-soluble DNA (digested sample/input)
0
10
20
30
40
50
60
0
5
12.5
25
50
Incubation time with DNase I (min)

Figure 2.3

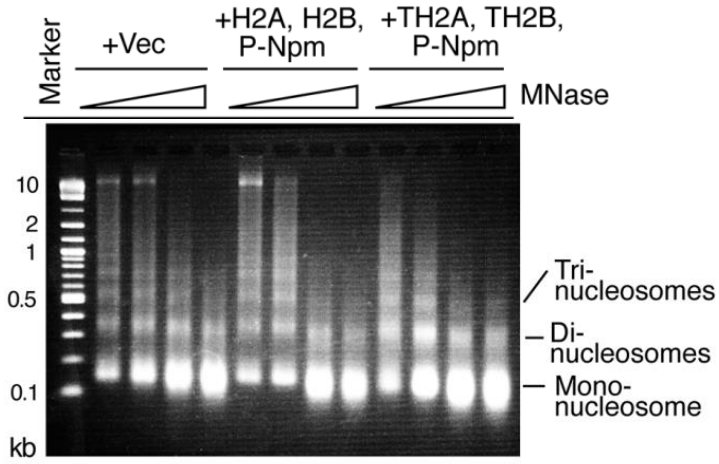
Marker
+Vec
+H2A, H2B, P-Npm
+TH2A, TH2B, P-Npm
MNase
10
2
1
0.5
0.1
kb
Tri-nucleosomes
Di-nucleosomes
Mono-nucleosome

Figure 2.4

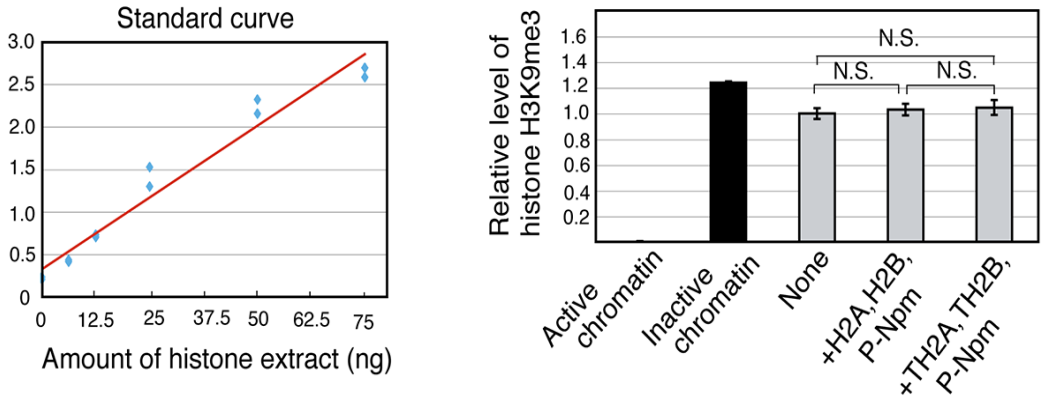
O.D. 450
Standard curve
3.0
2.5
2.0
1.5
1.0
0.5
0
0
12.5
25
37.5
50
62.5
75
Amount of histone extract (ng)
Relative level of histone H3K9me3
1.6
1.4
1.2
1.0
0.8
0.6
0.4
0.2
N.S.
N.S.
N.S.
Active chromatin
Inactive chromatin
None
+H2A,H2B, P-Npm
+TH2A,TH2B, P-Npm

Figure 2.5

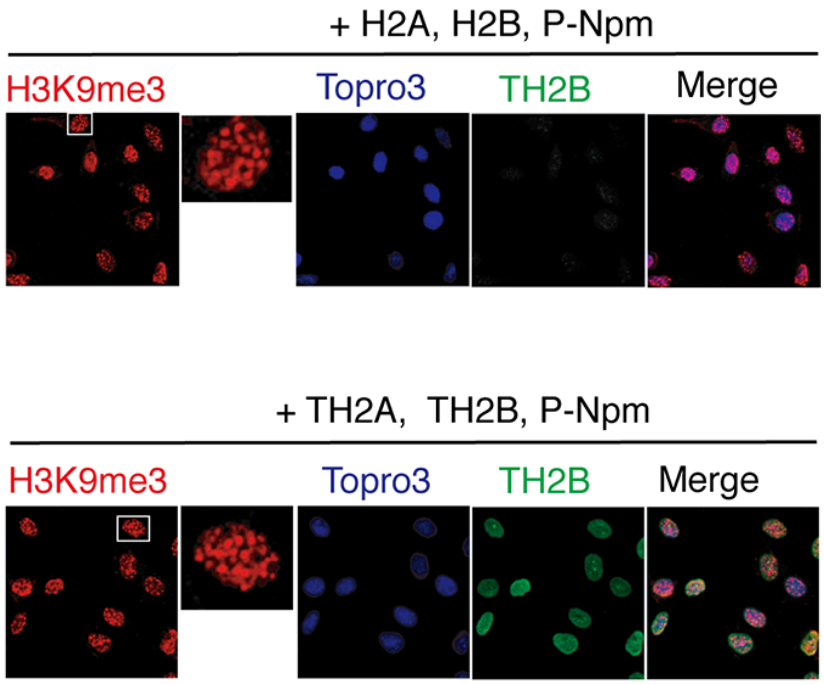
+ H2A, H2B, P-Npm
H3K9me3
Topro3
TH2B
Merge
+ TH2A, TH2B, P-Npm
H3K9me3
Topro3
TH2B
Merge

Figure 2.6

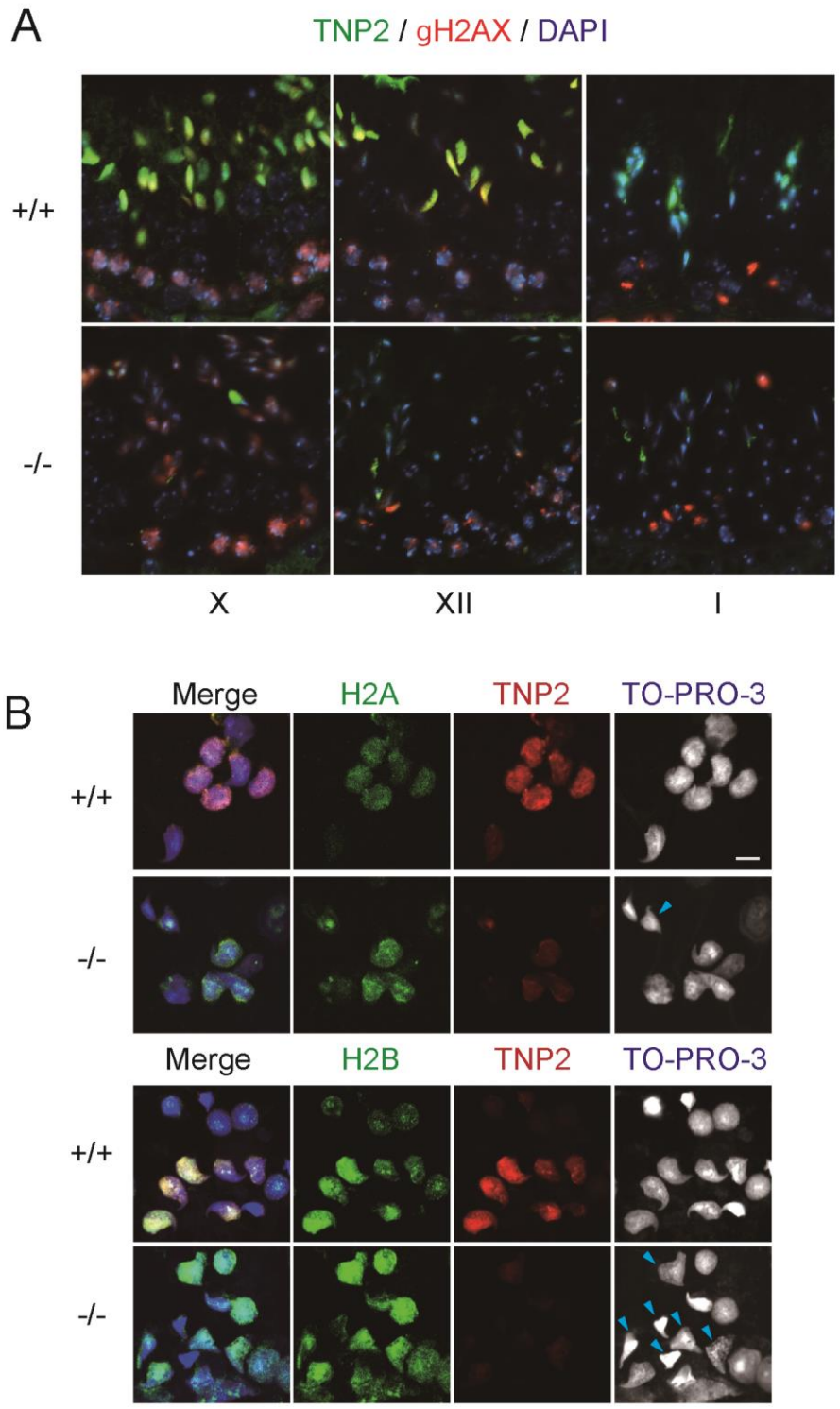
A
TNP2 / gH2AX / DAPI
+/+
-/-
X
XII
I
B
Merge
H2A
TNP2
TO-PRO-3
+/+
-/-
Merge
H2B
TNP2
TO-PRO-3
+/+
-/-

Figure 2.6

C

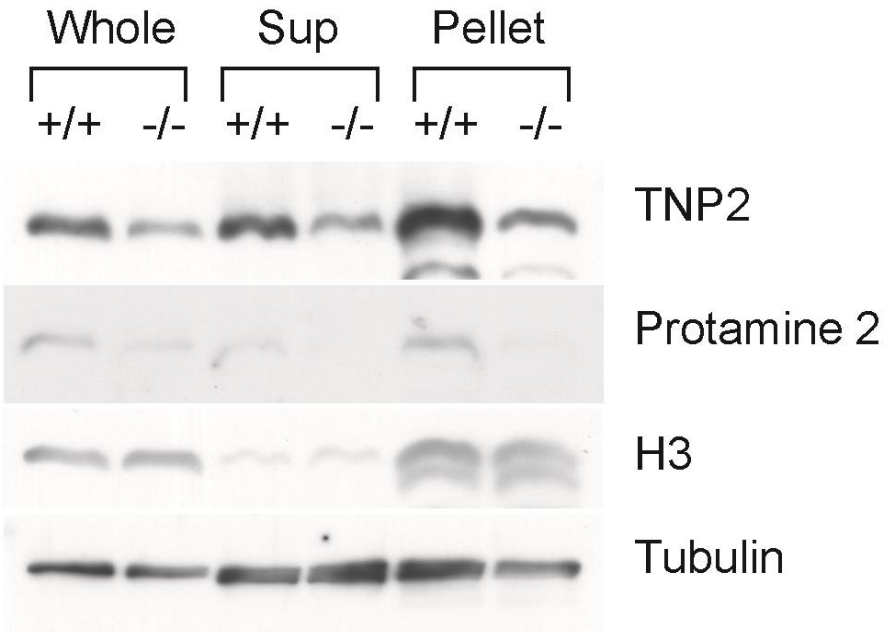

Figure 2.7

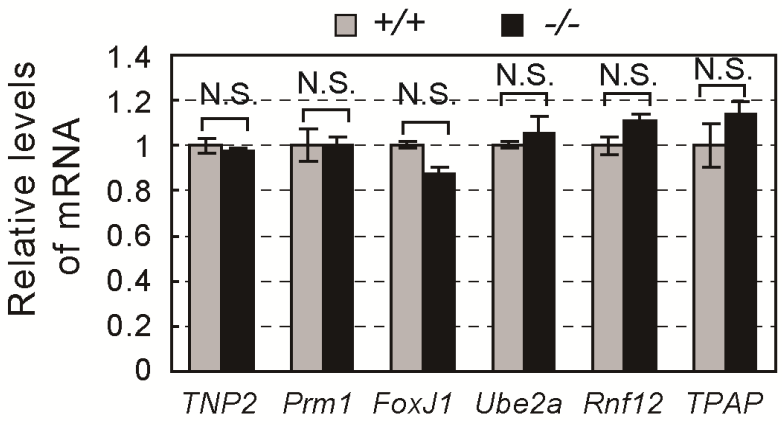
+/+
-/-
Relative levels of mRNA
1.4
1.2
1
0.8
0.6
0.4
0.2
0
N.S.
N.S.
N.S.
N.S.
N.S.
N.S.
TNP2
Prm1
FoxJ1
Ube2a
Rnf12
TPAP

Figure 2.8

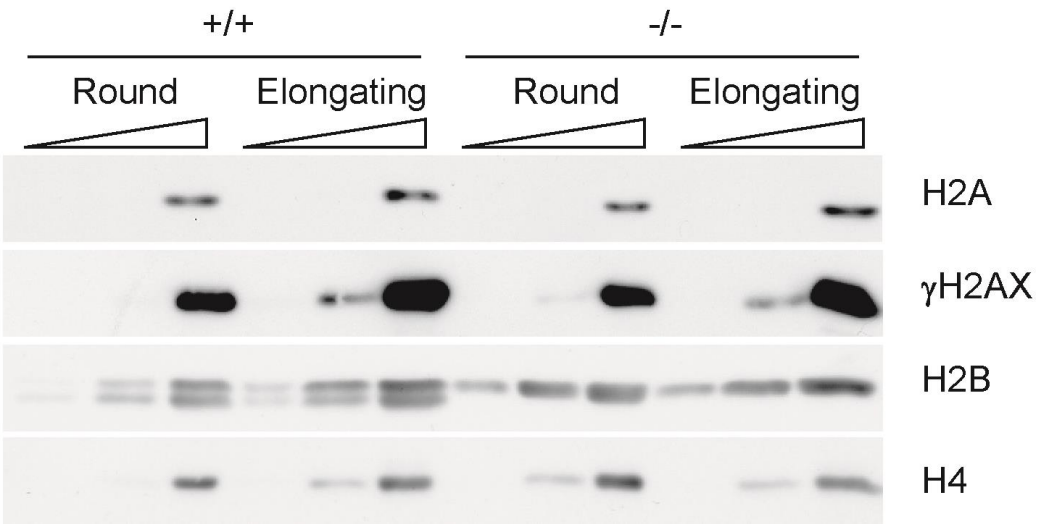

Figure 3.1

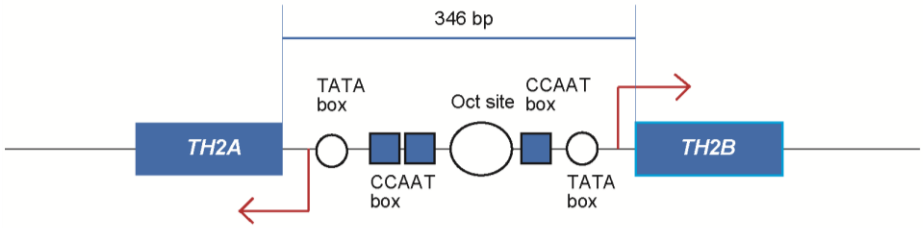


```
Canonical H2A   1   MSGRGKQGGKARAKAKTRSSRAGLQFPVGRVHRLLRKGNYSERVGAGAPVYLAAVLEYLT   60
Variant TH2A    1   MSGRGKQGGKARAKSKSRSSRAGLQFPVGRIHRLLRKGNYAERIGAGAPVYLAAVLEYLT   60

Canonical H2A   61  AEILELAGNAARDNKKTRIIPRHLQLAIRNDEELNKLLGRVTIAQGGVLPNIQAVLLPKK   120
Variant TH2A    61  AEILELAGNASRDNKKTRIIPRHLQLAIRNDEELNKLLGGVTIAQGGVLPNIQAVLLPKK   120

Canonical H2A   121 TES-HHKAKGK   130
Variant TH2A    121 TESHHHKAQSK   131

Canonical H2B   1   MPE-PAKSAPAPKKGSKKAVTKAQKKDGKKRKRSRKESYSVYVYKVLKQVHPDTGISSKA   59
Variant TH2B    1   MPEVSSKGATISKKGFKKAVVKTQKKEGKKRKRTRKESYSIYIYKVLKQVHPDTGISSKA   60

Canonical H2B   60  MGIMNSFVNDIFERIAGEASRLAHYNKRSTITSREIQTAVRLLLPGELAKHAVSEGTKAV   119
Variant TH2B    61  MSIMNSFVTDIFERIASEASRLAHYSKRSTISSREIQTAVRLLLPGELAKHAVSEGTKAV   120

Canonical H2B   120 TKYTSSK   126
Variant TH2B    121 TKYTSSK   127
```

Figure 3.2

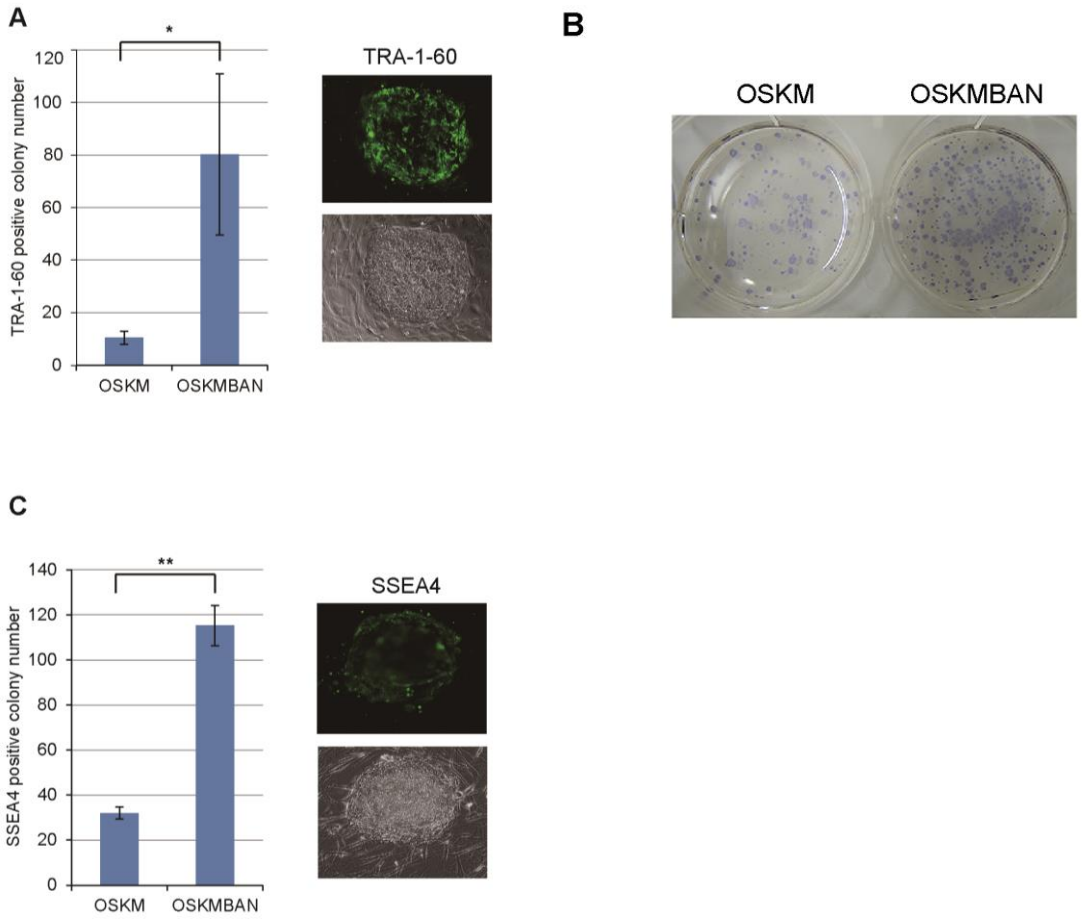
A
*
TRA-1-60 positive colony number
120
100
80
60
40
20
0
OSKM
OSKMBAN
TRA-1-60
B
OSKM
OSKMBAN
C
**
SSEA4 positive colony number
140
120
100
80
60
40
20
0
OSKM
OSKMBAN
SSEA4

Figure 3.3

A

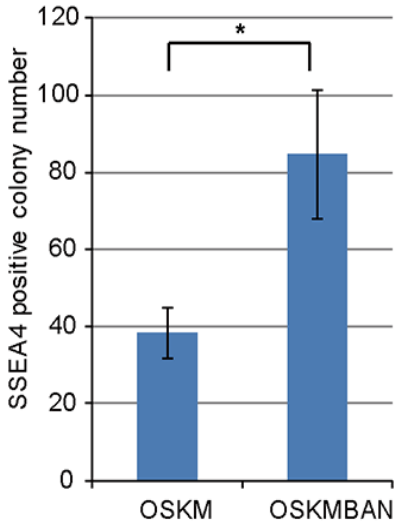
SSEA4 positive colony number
120
100
80
60
40
20
0
*
OSKM
OSKMBAN

B

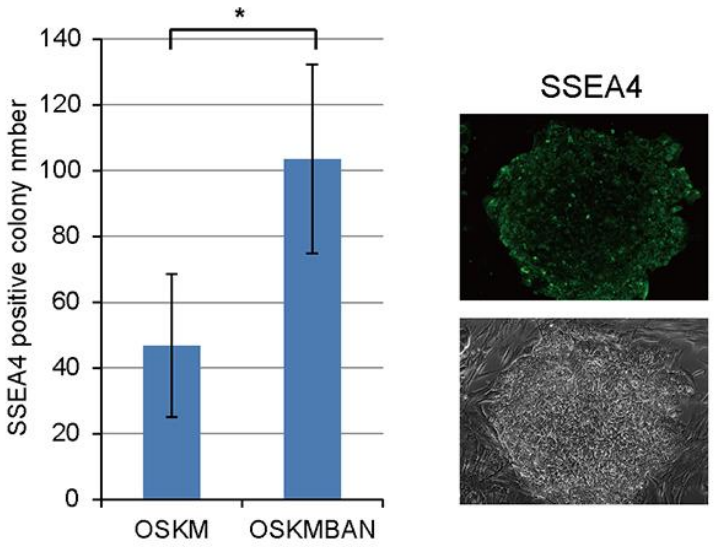
SSEA4 positive colony nmber
140
120
100
80
60
40
20
0
*
OSKM
OSKMBAN
SSEA4

Figure 3.4

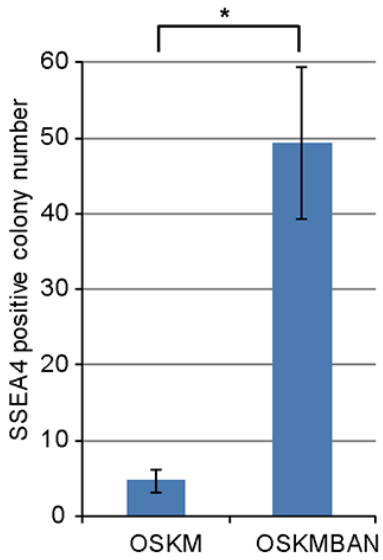

Figure 3.5

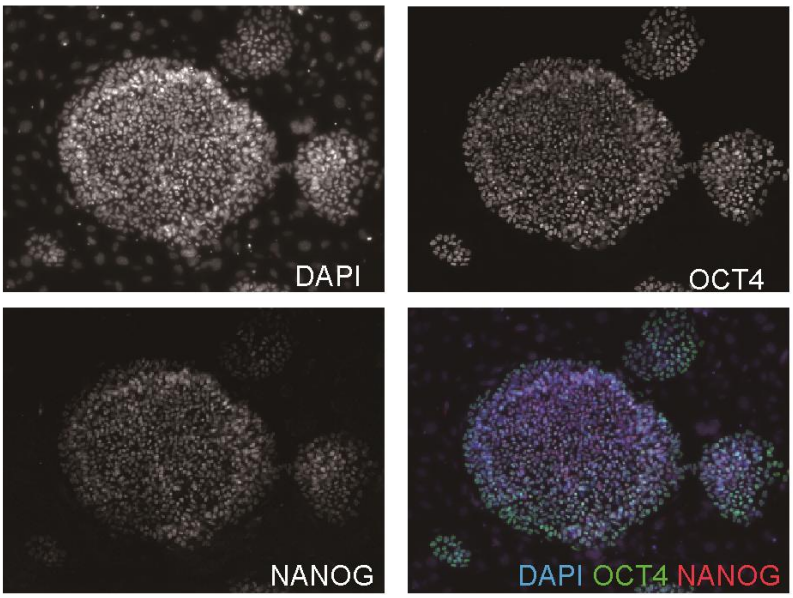

Figure 3.6

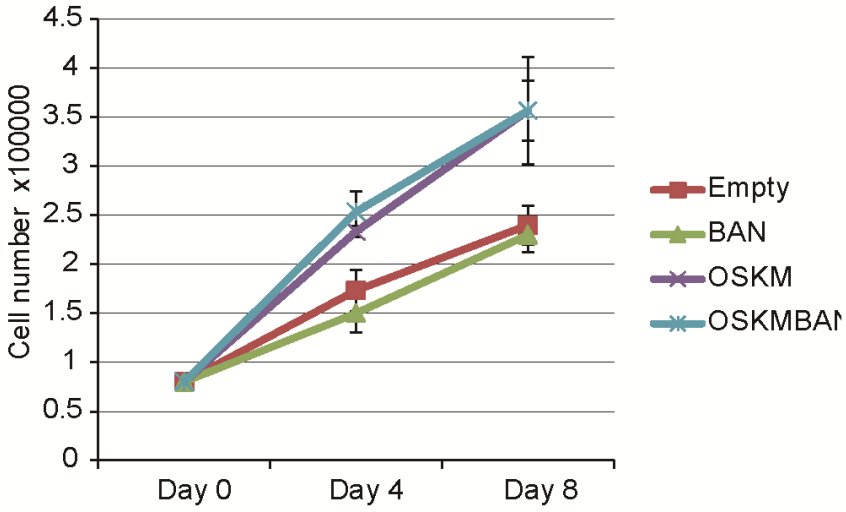
4.5
4
3.5
3
2.5
2
1.5
1
0.5
0
Cell number x100000
Day 0
Day 4
Day 8
Empty
BAN
OSKM
OSKMBAN

Figure 3.7

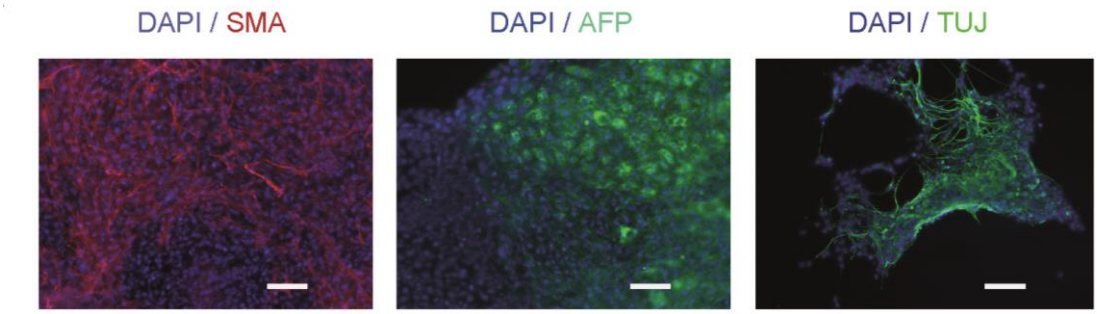

Figure 3.8

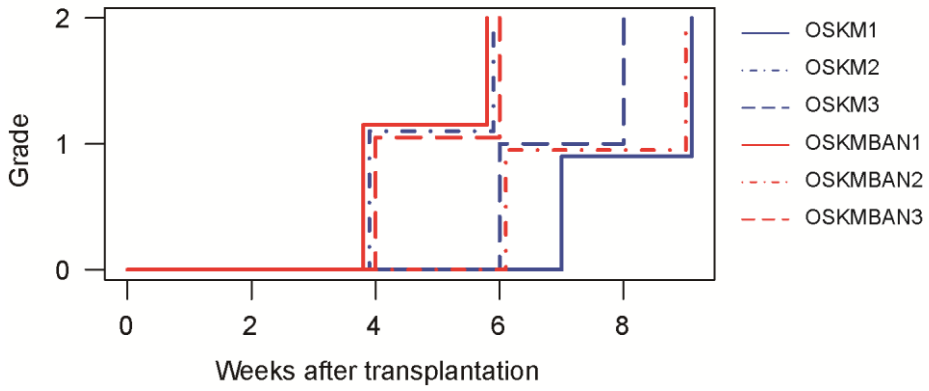
Grade
2
1
0
0
2
4
6
8
Weeks after transplantation
OSKM1
OSKM2
OSKM3
OSKMBAN1
OSKMBAN2
OSKMBAN3

Figure 3.9

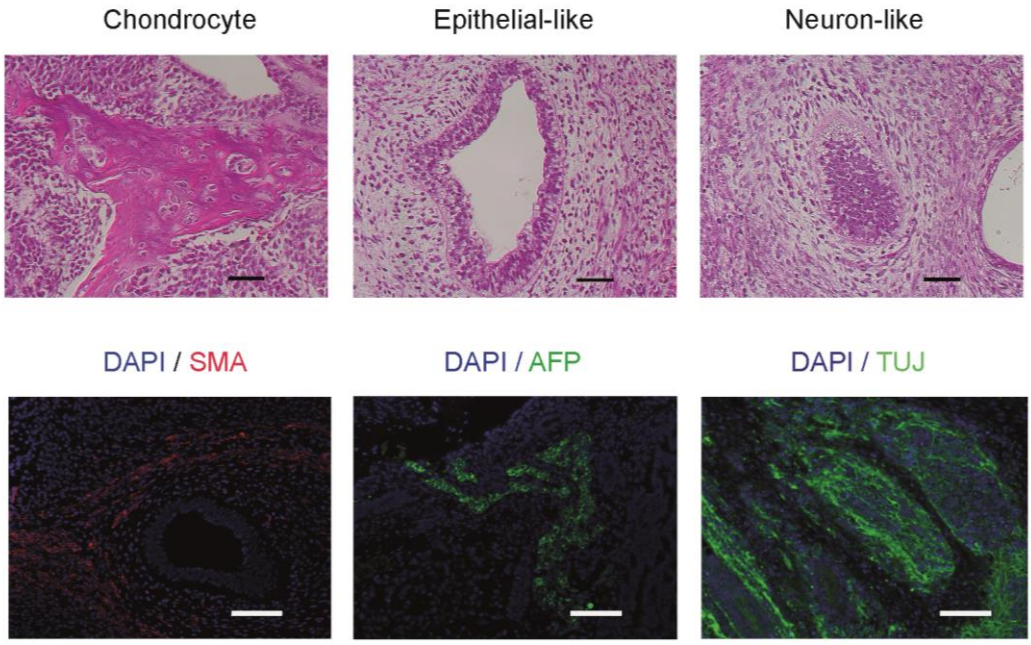
Chondrocyte
Epithelial-like
Neuron-like
DAPI / SMA
DAPI / AFP
DAPI / TUJ

Figure 3.10

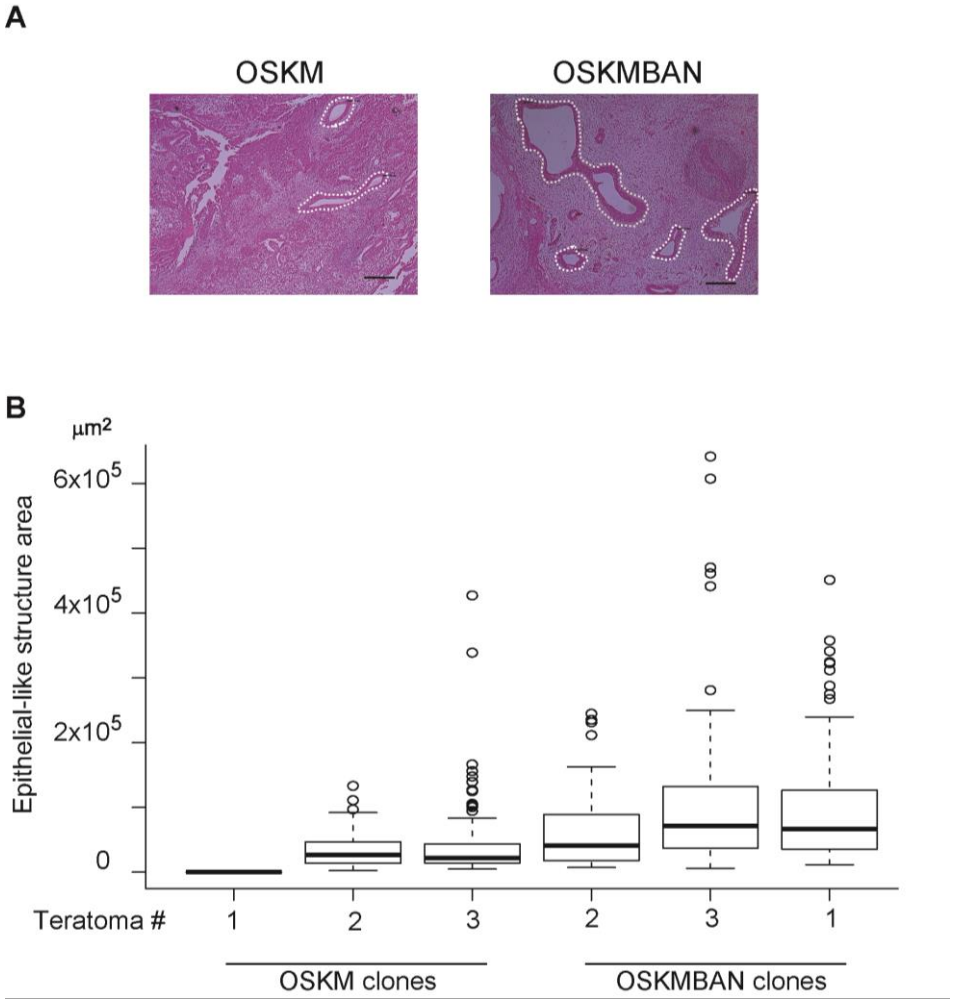
A
OSKM
OSKMBAN
B
µm²
6x10⁵
4x10⁵
2x10⁵
0
Epithelial-like structure area
Teratoma #
1
2
3
2
3
1
OSKM clones
OSKMBAN clones

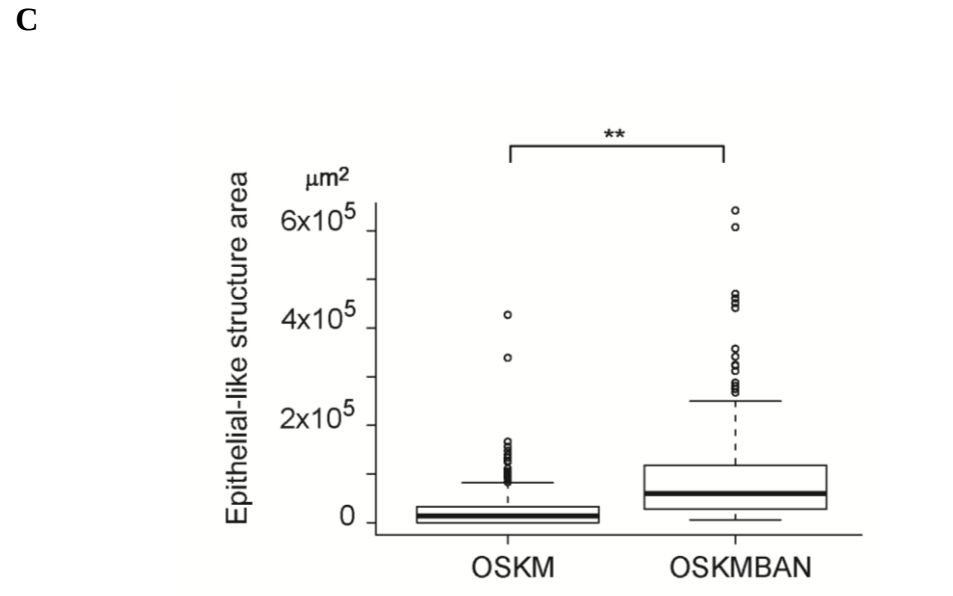
C
**
µm²
6x10⁵
4x10⁵
2x10⁵
0
Epithelial-like structure area
OSKM
OSKMBAN

Figure 3.11

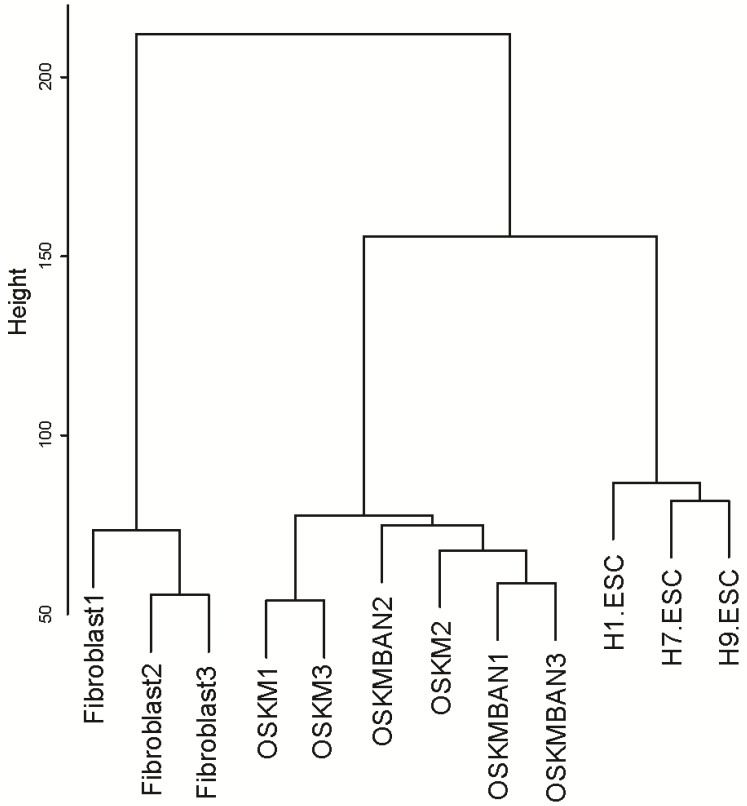
Height
200
150
100
50
Fibroblast1
Fibroblast2
Fibroblast3
OSKM1
OSKM3
OSKMBAN2
OSKM2
OSKMBAN1
OSKMBAN3
H1.ESC
H7.ESC
H9.ESC

Figure 3.12

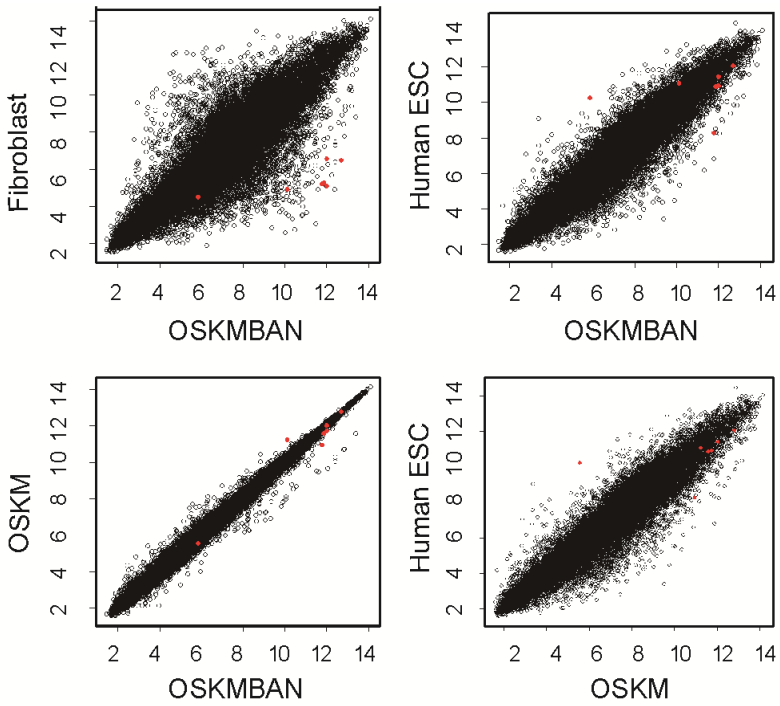
Fibroblast
OSKMBAN
Human ESC
OSKMBAN
OSKM
OSKMBAN
Human ESC
OSKM
2 4 6 8 10 12 14

Figure 3.13

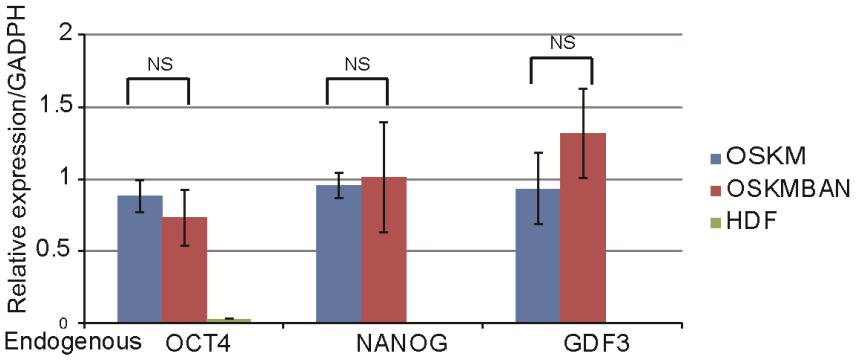
Relative expression/GADPH
2
1.5
1
0.5
0
NS
NS
NS
Endogenous
OCT4
NANOG
GDF3
OSKM
OSKMBAN
HDF

Figure 3.14

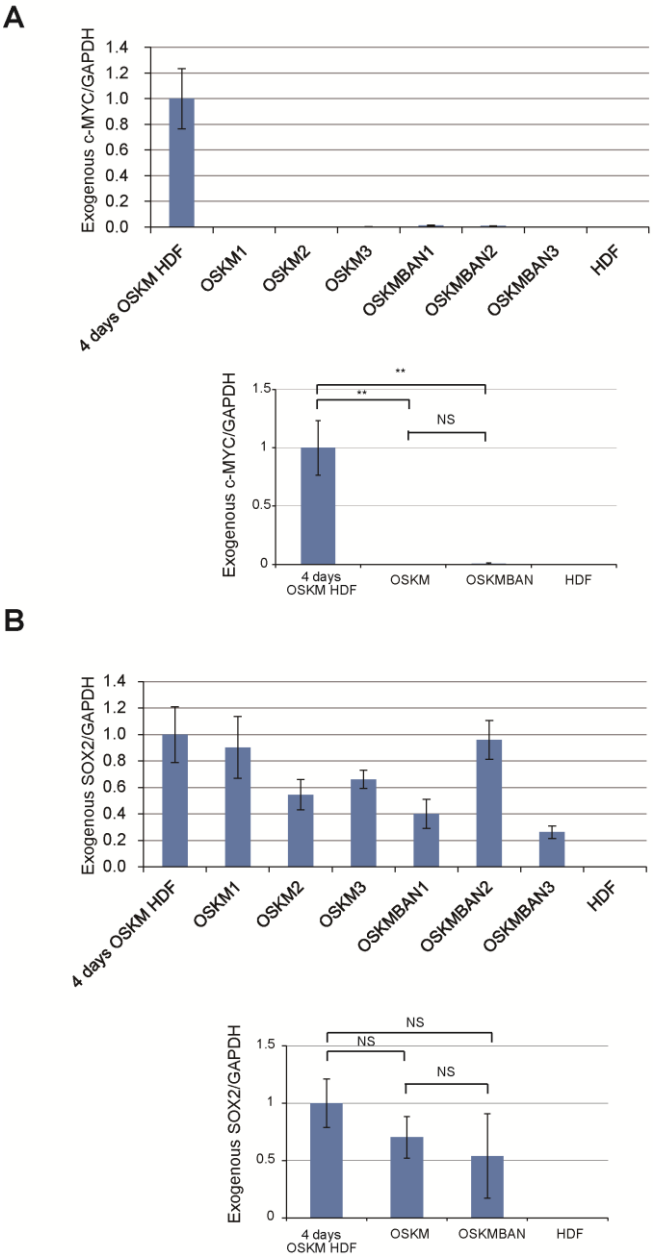
A
Exogenous c-MYC/GAPDH
1.4
1.2
1.0
0.8
0.6
0.4
0.2
0.0
4 days OSKM HDF
OSKM1
OSKM2
OSKM3
OSKMBAN1
OSKMBAN2
OSKMBAN3
HDF
**
**
NS
1.5
1
0.5
0
4 days OSKM HDF
OSKM
OSKMBAN
HDF
B
Exogenous SOX2/GAPDH
1.4
1.2
1.0
0.8
0.6
0.4
0.2
0.0
4 days OSKM HDF
OSKM1
OSKM2
OSKM3
OSKMBAN1
OSKMBAN2
OSKMBAN3
HDF
NS
NS
NS
1.5
1
0.5
0
4 days OSKM HDF
OSKM
OSKMBAN
HDF

Figure 3.15

KEGG Pathway	NES	p-value	FDR q-val
OLFACTORY TRANSDUCTION	2.279	<0.001	<0.001
DRUG METABOLISM CYTOCHROME_P450	1.922	<0.001	0.002
METABOLISM OF XENOBIOTICS BY CYTOCHROME P450	1.894	<0.001	0.004
RETINOL METABOLISM	1.684	<0.001	0.046
GLYCOLYSIS GLUCONEOGENESIS	1.671	0.004	0.044
DRUG METABOLISM OTHER ENZYMES	1.650	0.009	0.047
CYTOKINE CYTOKINE RECEPTOR INTERACTION	1.597	<0.001	0.074
JAK STAT SIGNALING PATHWAY	1.549	0.004	0.097

Figure 3.16

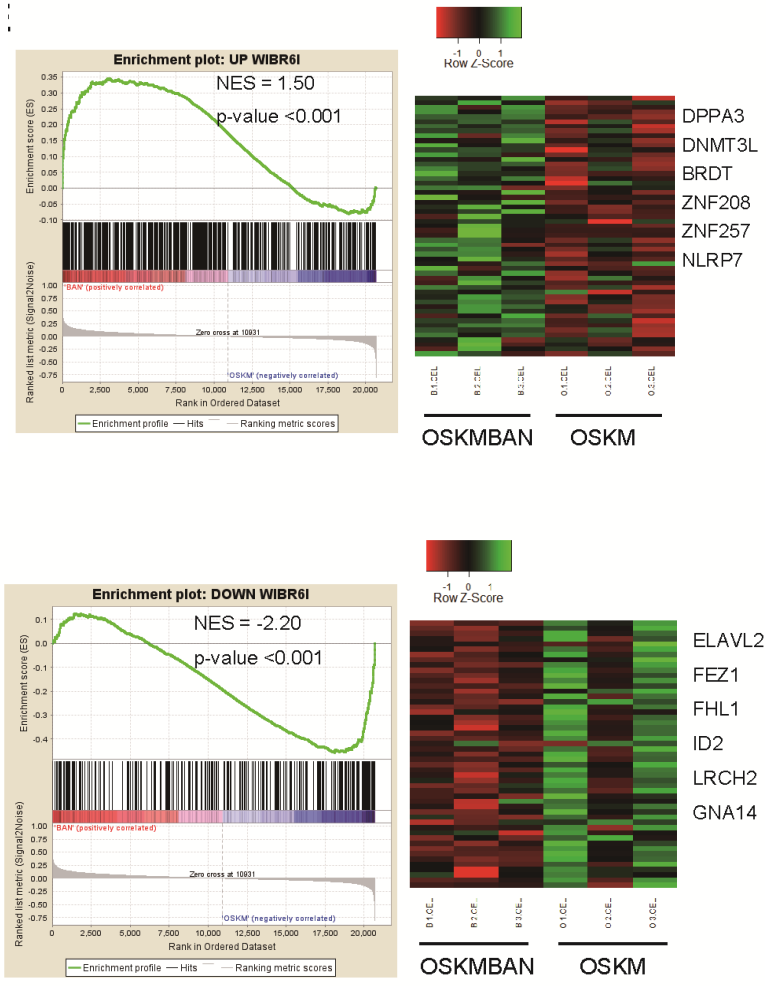
Enrichment plot: UP WIBR6I
NES = 1.50
p-value <0.001
Enrichment score (ES)
'BAN' (positively correlated)
Zero cross at 10931
'OSKM' (negatively correlated)
Ranked list metric (Signal2Noise)
Rank in Ordered Dataset
Enrichment profile
Hits
Ranking metric scores
Row Z-Score
DPPA3
DNMT3L
BRDT
ZNF208
ZNF257
NLRP7
OSKMBAN
OSKM
Enrichment plot: DOWN WIBR6I
NES = -2.20
p-value <0.001
ELAVL2
FEZ1
FHL1
ID2
LRCH2
GNA14